FINAL DEGREE PROJECT

Electrical Engineering Degree

DESIGN AND OPTIMIZATION OF A PERMANENT MAGNET SYNCHRONOUS MACHINE

Memory and annexes

Author: Matias Fernando Richter
Director: Ramón Bargalló Perpiñà
Date: Enero 2018

1. Abstract

The purpose of the present project is the design and optimization of a fifth teen-slot ten pole permanent magnets synchronous machine with interior magnets and concentrated windings. Stator and rotor armatures are taken from an existing motor of different characteristics, which is actually in production.

The main motivation of building different types of motors with the same materials is to reduce the costs and to simplify the production process, increasing at the same time, the variety of products offered.

The start points are the needed characteristics and the existing motor. The stator and rotor armatures are taken, modifying slightly the rotor frame in order to reduce the cogging torque and to optimize the motor operation. Then, the calculations of the design parameters are made, and finally the simulations to obtain the motor characteristics.

The project contains a memory, which describes the followed methodology to study and design the motors, with theoretical explanations of the calculations y simulations performed. It also contains annexes of the calculations done, their justifications and the results obtained.

UNIVERSITAT POLITÈCNICA DE CATALUNYA
BARCELONA**TECH**
Escola d'Enginyeria de Barcelona Est

2. Resumen

El presente proyecto tiene como objetivo el diseño y la optimización de un motor de quince ranuras y diez polos, de imanes permanentes interiores y bobinado concentrado, partiendo de la base de una chapa y un rotor utilizado en un motor actualmente en producción.

La reducción de costes y simplificación en el proceso de producción son los motivos por los cuales se busca construir diferentes gamas de motores con la misma base de materiales, al tiempo que se incrementa la cantidad de productos que se ofrecen.

El punto de partida son unas deseadas características y un motor existente y en cadena de producción, del cual se toman la chapa del estator y del rotor, modificando levemente el diseño del rotor para reducir el par de "cogging" y optimizar su funcionamiento. A partir de aquí, se realizan los cálculos de los parámetros de diseño deseados y se realizan las simulaciones correspondientes para la obtención de las características del motor.

El proyecto consta de una memoria descriptiva de la metodología seguida para el estudio y diseño del motor, con explicaciones teóricas de los cálculos y simulaciones realizadas. Se presentan también anexos de los cálculos realizados, su justificación y los resultados obtenidos.

UNIVERSITAT POLITÈCNICA DE CATALUNYA
BARCELONA**TECH**
UPC   Escola d'Enginyeria de Barcelona Est

3. Resum

El present projecte té com a objectiu el disseny i l'optimització d'un motor de quinze ranures i deu pols, d'imants permanents interiors i bobinatge concentrat, partint de la base d'una xapa i un rotor utilitzat en un motor actualment en producció.

La reducció de costs i simplificació en el procés de producció són els motius pels quals es busca construir diferents gammes de motors amb la mateixa base de materials, al mateix temps que s'incrementa la quantitat de productes que s'ofereixen.

El punt de partida són unes desitjades característiques i un motor existent i en cadena de producció, del com es prenen la xapa de l'estator i del rotor, modificant lleument el disseny del rotor per reduir el parell de "cogging" i optimitzar el seu funcionament.. A partir d'aquí, es realitzen els càlculs dels paràmetres de disseny desitjats i es realitzen les simulacions corresponents per a l'obtenció de les característiques del motor.

El projecte consta d'una memòria descriptiva de la metodologia seguida per a l'estudi i disseny del motor, amb explicacions teòriques dels càlculs i simulacions realitzades Es presenten també annexos dels càlculs realitzats, la seva justificació I els resultats obtinguts.

UNIVERSITAT POLITÈCNICA DE CATALUNYA
BARCELONATECH
Escola d'Enginyeria de Barcelona Est

UNIVERSITAT POLITÈCNICA DE CATALUNYA
BARCELONATECH
Escola d'Enginyeria de Barcelona Est

4. Acknowledgements

UNIVERSITAT POLITÈCNICA DE CATALUNYA
BARCELONA**TECH**
Escola d'Enginyeria de Barcelona Est

Index

UNIVERSITAT POLITÈCNICA DE CATALUNYA
BARCELONA**TECH**
Escola d'Enginyeria de Barcelona Est

UNIVERSITAT POLITÈCNICA DE CATALUNYA
BARCELONA**TECH**
Escola d'Enginyeria de Barcelona Est

UNIVERSITAT POLITÈCNICA DE CATALUNYA
BARCELONATECH
Escola d'Enginyeria de Barcelona Est

x

1. Introduction

Day to day, the Permanent Magnets Synchronous Machines (PMSM) are more used in all environments. This is due the improvement in control methods with new technologies of power electronics, and to the development of better permanent magnets, such as the Neodymium, known as rare-earth magnets. PMSM have a higher power density, this is power per weight unity, and better efficiency than conventional machines because there are no losses in the inductor copper. This is why it is very interesting the development of PMSM.

1.1. Work objectives

The main objective of this work is to design a PMSM from existing stator and rotor armatures to develop the desired characteristics, and at the same time, to optimize the operation of the motor.

1.2. Scope and methodology

The present work includes the analytical calculations to approximate the design of the machine done in the software MathCAD. The pre-design simulation in the software JMAG to confirm the desired characteristics, with the parameters obtained with the calculations. The simulations performed with the software FEMM, "Finite Element Method Magnetics", to obtain all the machine parameters and characteristics. It includes also an economical study and budget of the production costs.

2.   Permanent Magnets Synchronous Machines

2.1.   The Synchronous Machine

The synchronous machines are all the electric machines whose rotation speed is strictly constant and depends directly from the frequency of the AC power supply system applied. They follow directly the expression:

$$N = \frac{60\,f}{p}$$

(1.1)

Where:

N: Synchronous rotation speed [rpm]

f: Frequency of the AC supply [Hz]

p: Pair of magnetic poles of the machine

So the speed depends directly from the frequency and the number of poles of the machine. The different speed possibilities for different numbers of poles and for the two main supply frequencies (50 and 60Hz) are shown on the next tables:

Frequency	50					
Pair of Poles	1	2	3	4	5	6
Speed	3000	1500	1000	750	600	500

Frequency	60					
Pair of Poles	1	2	3	4	5	6
Speed	3600	1800	1200	900	720	600

UNIVERSITAT POLITÈCNICA DE CATALUNYA
BARCELONA**TECH**
Escola d'Enginyeria de Barcelona Est

As all electromechanical converters, they can work as a motor or as a generator ("Electromagnetic reciprocity principle"). They are usually employed as generators in the electric centrals (hydraulic, thermic, nuclear) and on a minor scale, they are used in generators sets, as emergency supply systems in hospitals, airports, etc, in case of failure of the main supply. The synchronous motors are used in industrial processes mainly in those that required a constant speed.

2.2. Basic construction aspects

There are many possible configurations in the construction of a synchronous machine. The main construction aspect of the synchronous machine is to build the stator with windings which are fed with an AC power supply, and to have in the rotor the concentrated windings fed with DC current, which create the magnetic poles of the machine. -The PMSM has permanent magnets (PM) usually in the rotor to create the poles.

This is how they are usually constructed, but as mentioned before, there are any different configurations, as an example, on low power machines, the DC created poles could be on the stator and the AC windings on the rotor:
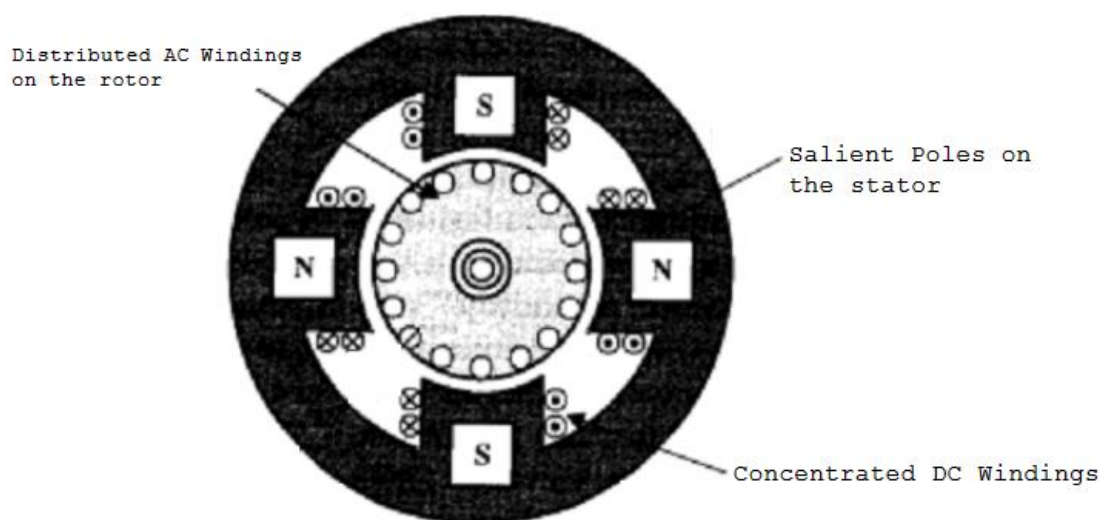

Figure 1.1 – Low Power Synchronous Machine. Induced windings on the rotor

Analyzing the usual construction configuration in which the induced AC windings are in the stator, they can adopt two main ways of construction: Salient or Non-Salient poles.
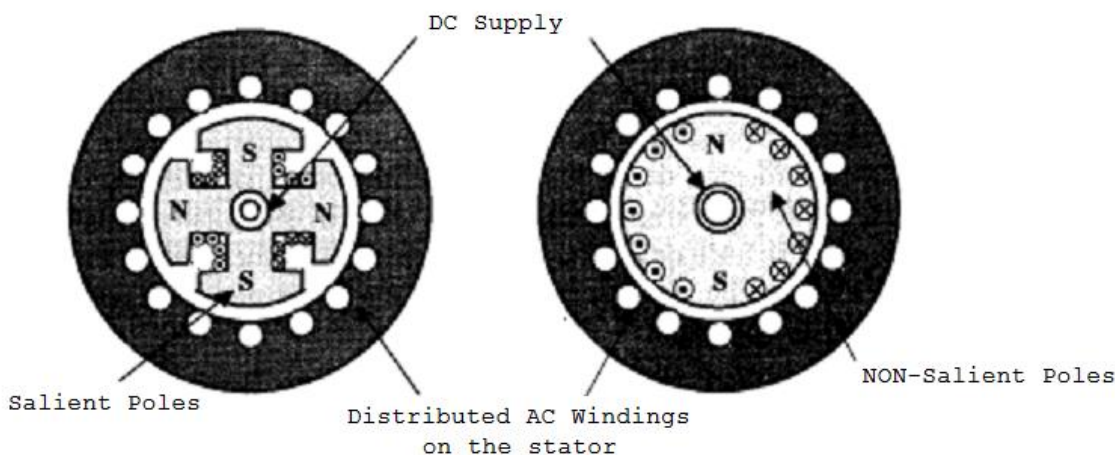
Figure 1.2 –Salient and NON-Salient Poles Synchronous Machine. Induced Windings on the stator

As it can be observed on the Figure 1.2, the inductor windings on the Salient Poles configuration create two pair of poles and they are concentrated. On the NON-Salient configuration, the inductor windings are distributed along the rotor creating one pair of poles.

The main difference between these two configurations is the working speed of the machine. So to choose one or another we have to estimate the needed rotation speed of the application. For high rotation speeds, the NON-Salient Poles configuration is usually chosen. For example the Turbo generators are moved by vapor turbines and their rotation speed is really high. So they are normally built with a NON-Salient poles configuration. One of the reasons is the centrifugal force generated by high speeds, so they are built with a short diameter and a long axial longitude. Salient Poles configuration is normally used in low speed applications and built with a large number of poles. Usually their axial longitude is shorter than their diameters. The hydraulic generators are usually built with salient poles.

2.3. Working principles

When we think about the working principle of an electrical machine, we think actually how torque is generated. The synchronous machine has the induced windings on the stator and when they are fed with an AC supply, an oscillatory magnetic field is created. These oscillations because of the AC Supply can be represented as a rotating field:
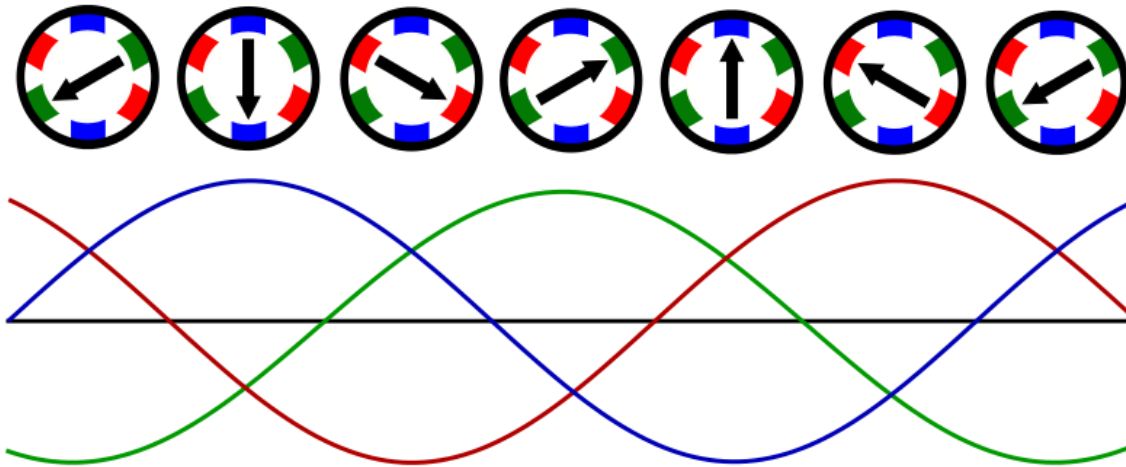
Figure 1.3 –Rotating magnetic field created on the stator because of the 3-Phase AC Supply

In the rotor is the inductor circuit that creates the poles of the machine by the DC current, or in our case, by the permanent magnets. The static magnetic field of the permanent magnets in the rotor aligns and locks the orientation with the rotating magnetic field of the stator. In the synchronous machines, the magnetic field is always solidary to the rotor. So if the magnetic field of the stator rotates, the rotor will follow the rotation at the same synchronous speed because the fields are magnetically locked.
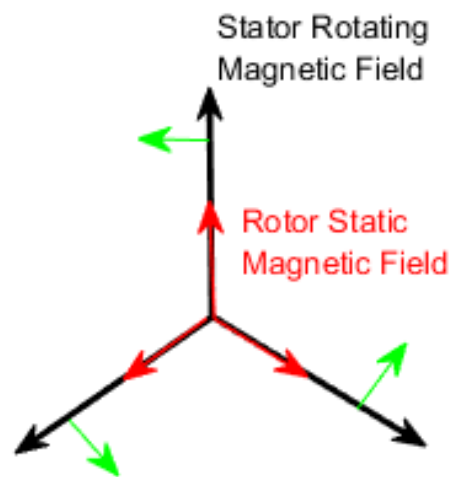
Figure 1.3 – Stator rotating magnetic field (black) and rotor static magnetic field (red). It locks on the same orientation and rotates at synchronous speed

On the next figure can be observed how torque is generated by the AC Supply on the stator. The current of the stator windings create the rotating magnetic field. Depending on the direction of the current on each conductor in each time period, a North or a South Pole is generated and the field of the rotor aligns himself in this direction. With the properties of vectorial products (or the "Right-hand Rule") is not difficult to determine the torque generated: the direction of the current and the induction (B) generates a force F (Torque).
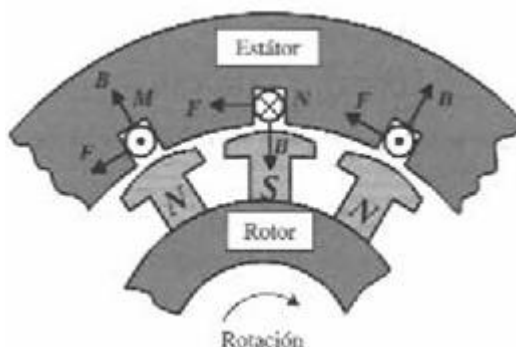
Figure 1.5 —Stator conductors create a rotating magnetic field. Rotor static magnetic field aligns with the rotating field.

On the next cycle the currents will revert their directions, creating the opposite poles on the same place, and because the rotor is rotating at synchronous speed, the fields will be again aligned, and a torque force is generated again on the same direction.

2.4. Generating Torque at zero speed

So as explained before, the machine creates the torque by locking the rotor magnetic field to de rotating stator field. But for that to be possible, the rotor must be already rotating, and the mechanical speed and the rotating magnetic field speed must be the same: the synchronous speed. The synchronous machine only creates torque on the same direction at the synchronous speed.

Synchronous machines cannot start by them self's, because the net torque generated after a whole period is zero. Same happens when the speed is not exactly the synchronous speed: torque generated changes direction, and machine could be stopped because it desynchronizes.

Next figure explains graphically how at non synchronous speed the net torque is zero.
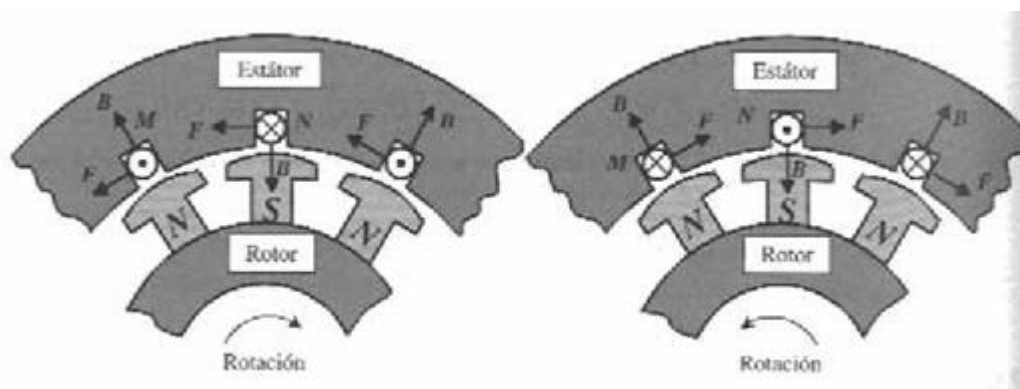
Figure 1.6 – Synchronous Machine cannot generated torque at zero speed

On the left of Figure 1.6 can be seen the first semi-cycle of the period. The direction of the current and the induction, aligned with the rotor poles, generate the torque in one direction: Rotation: clockwise. On the next semi-cycle (right figure), when the currents invert their directions, the rotor must align with the stator field, but because of the mechanical inertia of the rotor and mechanical friction, the rotor is not able to follow the magnetic field instantly at the same speed, and torque is generated but in opposite direction: Rotation: anti-clockwise. So the net torque at the end of the period is zero. Resuming, at non-synchronous speeds, and at zero speed, the torque generated changes the direction resulting in the whole period a net torque generated equal to zero. Starting process of these motors is done normally driven with an electronic control, fed with an electronic inverter.

2.5. Permanent Magnet Synchronous Machine

The PMSM is a synchronous machine with the only constructive difference, that the inductor DC circuit is replaced by permanent magnets. In the next figure are represented three of the usual possible variations of the magnets configuration on the rotor.

Figure 1.7 –a) Salient Poles (Surface-mounted); b) NON-Salient Poles(Inset); c)Interior Permanent Magnet rotor

The magnetic flow of the excitement circuit, located on the rotor, cannot be change, because naturally, in the permanent magnet the field is constant. So it cannot be controlled, but instead, there are no losses in the rotor, because there are no windings. So taking into account that the main losses of a machine are the Joule Losses, and these ones are proportional to the square of the current, if we avoid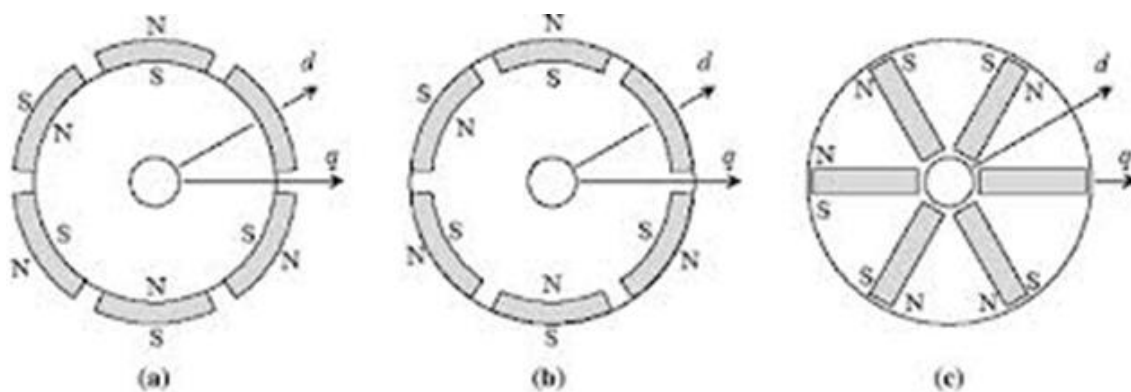 having an excitement circuit, we are reducing a lot the losses and increasing a lot the efficiency of the machine. This is one of the most important reasons to understand why Permanent Magnets Machines are so interesting. At the same time, with fewer losses, heat is lower, so no need to developed complicated dissipation and insulating systems. And it can work on a bigger range of temperatures.

The emergence of new powerful magnetic materials, such as neodymium, has brought the possibility of development of new PMSM motors, which, compared to asynchronous machines, can generate same power and torque in the same, even less volume, because the magnets occupy much less volume than the windings needed to create the same magnetic field. In other words, the torque density is much higher than in Induction Machines, PMSM need smaller frame size to generate same power.

One of the bigger disadvantages of the PMSM is obviously, that it is not possible to control the excitation circuit. This remains constant because of the magnets. So for example working as generators, the reactive power cannot be adjust by regulating the excitation circuit. The output voltage depends directly from the load, and the power factor of the load must be regulated by installing condensers. Same happens with the torque ripple. Torque is not smooth, because excitation cannot be controlled, and it appears the cogging torque, due to the interaction of the magnets with the stator teeths.

Nowadays, the main applications for these motors are working as servomotors in robotics, motors for lifts or in the automotive industry. In this field the PMSM are getting a lot of importance, because

they are being installed in all the new electric or hybrid cars. Usually these kinds of motors are all controlled by a rectifier-inverter group and different control methods, such as Field Oriented Control "FOC" or Direct Torque Control "DTC".

3. Initial Design Data

3.1. Main characteristics

The main objective of this work is to design a PMSM from existing rotor and stator armatures from a motor which is actually being produced. The desired characteristics are a nominal power of 2,2 kW and rated speed 1500 rpm. The efficiency must be at least 91,4%, according to the IEC 60034-30 and the power factor 0,8. The motor is going to be fed with a rectifier-inverter group, from a three phasic 230 line voltage.

Design Characteristics	
Power	2,2 kW
Rated Speed	1500 rpm
η	91,40%
cos φ	0,8

3.2. Armatures

The idea of taking existing armatures to design a new type of motor is to have the possibility of building motors of different characteristics but with the same material and pieces. In this case, the existing armatures are a 15 slot stator and a 10 PM pole rotor, shown on the next figures. The material used is the steel M470 50A, thickness 1mm.

UNIVERSITAT POLITÈCNICA DE CATALUNYA
BARCELONA**TECH**
Escola d'Enginyeria de Barcelona Est
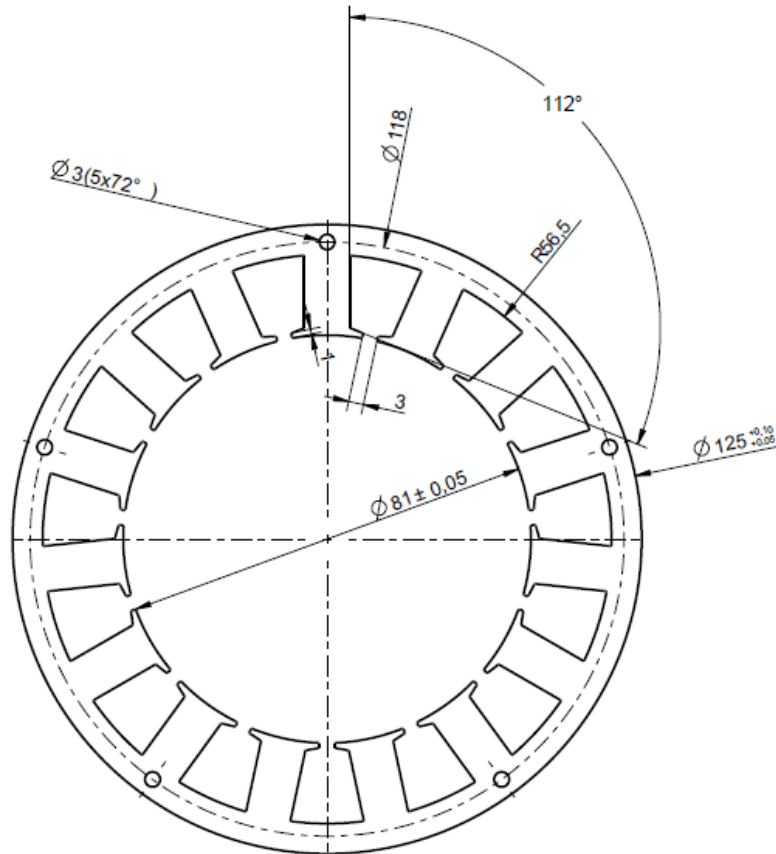
Figure 2.1 – Stator armature. Details on Annex D

UNIVERSITAT POLITÈCNICA DE CATALUNYA
BARCELONATECH
Escola d'Enginyeria de Barcelona Est
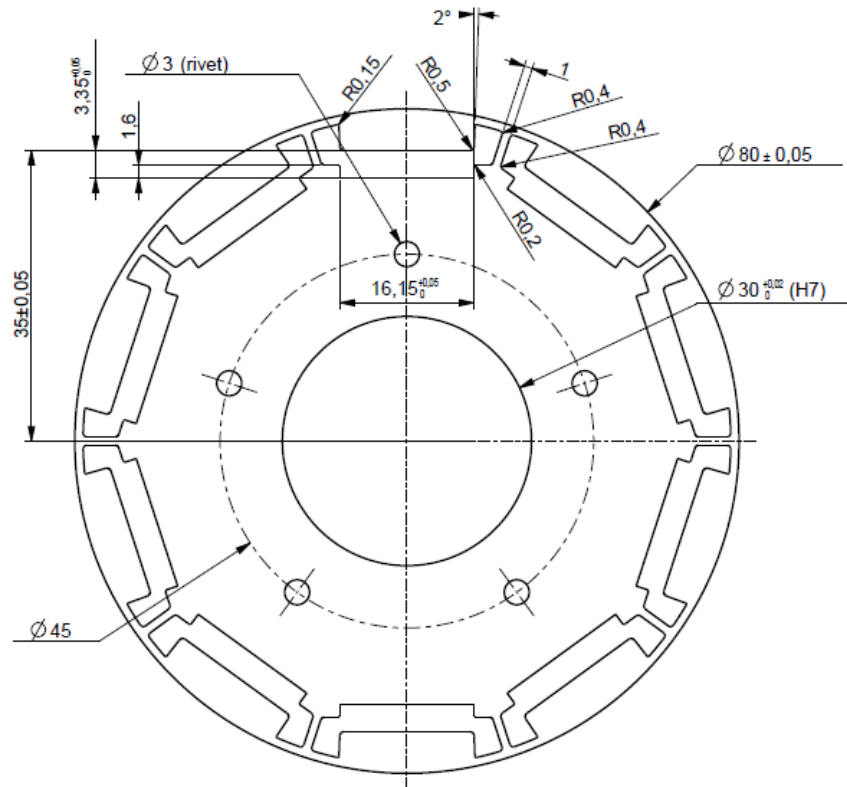
Figure2.2 – Rotor armature. Details on Annex D

In order to optimize the design and the motor efficiency, the rotor armature will be slightly modify, by changing the angle of the air slot, achieving an important decrease of the cogging torque generated by the permanent magnets. Process and results are described in chapter 6.2.

On the next table are described the armatures main characteristics.

	Stator	Rotor
Slots / Poles	15	10
Outer Diameter [mm]	125	80
Inner Diameter / Shaft [mm]	81	30
Thickness [mm]	1	1

Table 2.1 – Armature main characteristics

4. Initial Calculations

It is necessary to start the design by doing some analytical calculations in order to approximate the main characteristics. The goal is to obtain the values to star the design with and to not oversize the design. In most cases these calculations help only to approach a parameter value, which is later in the simulations determined. The start point are the nominal working conditions of the machine.

The mathematical model used is based on the following assumptions:

- The stator windings are balanced with sinusoidal distributed magneto-motive force.

- The inductance distribution in the air gap is sinusoidal.

- The saturation and parameter changes are neglected.

- The three-phase machine is assumed to have a balances supply system.

4.1. Rated Conditions

4.1.1. Torque

The nominal torque (Mn) will be generated when the machine works at nominal speed (Nn) giving the nominal power (Pn). Situation described with the expression:

$$M_n := \frac{P_n}{\left(\frac{2 \cdot \pi}{60}\right) \cdot N_n}$$

[1.1]

4.1.2. Synchronous Frequency

The machine is going to be fed with a rectifier-inverter equipment. It will allow to control the operation points of the motor. If there were no power electronics involved, the motor would rotate at the synchronous speed (speed depends on the poles of the machine) generated by the frequency of the power supply system, normally 50 Hz. So to achieve the rated speed of the machine, it needs to be fed with a frequency according to the poles of the machine:

UNIVERSITAT POLITÈCNICA DE CATALUNYA
BARCELONATECH
Escola d'Enginyeria de Barcelona Est

$$fs := p \cdot \frac{N_n}{60} =$$

[1.2]

Where "p" refers to the pair of poles of the machine. In our case: 10 poles → p=5.

4.1.3. Current

The rated current of the machine depends directly of the supply voltage, and because it has a star connection, the voltage needs to be the phase voltage:

$$U_n := \frac{230}{\sqrt{3}}$$

[1.3]

The line peak voltage will be:

$$U_{lmax} := 230 \cdot \sqrt{2}$$

[1.4]

The expression that determines the rated current of the machine is:

$$In := \frac{P_n}{m \cdot U_n \cdot \eta \cdot \cos\varphi}$$

[1.5]

Where "m" refers to the number of phases of the power supply system. In our case: 3

4.2. Machine Dimensions

Once the main rated parameters are calculated, it can be estimated the dimensions of the machine. The diameter of the machine is fixed by the armature chosen. So, the stack length needs to be calculated for the specified desired characteristics.

The expression used to determine the stack length relates the poles and the nominal power with the number of phases of the supply system (m), the current layer (As), the average induction (Bav), the efficiency (η), the synchronous frequency (fs) and the outer stator diameter (De). It is also affected by waveforms coefficients.

$$L := \frac{2 \cdot p \cdot P_n}{m \cdot A_s \cdot K_e \cdot K_i \cdot K_p \cdot D_e^{\,2} \cdot \eta \cdot B_{av} \cdot \pi \cdot f_s}$$ [1.6]

4.2.1. Current layer

The current layer is the uniformed distribution of current that passes through an area, in the case of electric machines, the current that pass through the total of coils of the machine. The normal values for rotating electric machines are between 750 and 35000 A/m.

4.2.2. Permanent magnets dimensions

The magnet dimensions are determined by the existing rotor armature. The material used is NdFeB 40.

4.2.3. Average induction

The average induction in the air gap of the machine can be first estimated with the rated remain induction of the magnetic material used. The NdFeB 40 has a remain induction of 1,28 T, and the average induction can be estimated as a 70% of that value.

4.2.4. Waveform coefficients

The expression used to calculate the stack length of the machine is affected by three waveform coefficients because the waveforms of the model are sinusoidal, although it could be fed with other types of waveforms. These coefficients express the relationship between the MAX values and the RMS values of the signal for voltage (e), current (i) and power (p). The next table describes the waveforms and their coefficients.

UNIVERSITAT POLITÈCNICA DE CATALUNYA
BARCELONATECH
Escola d'Enginyeria de Barcelona Est

Model	e (t)	i (t)	K_i	K_p
sinusoidal			$\sqrt{2}$	$0.5\cos\varphi$
sinusoidal			$\sqrt{2}$	0.5
rectangular			1	1
trapezoidal			1.134	0.777
triangular			$\sqrt{3}$	0.333

Figure 4.1 – Waveforms coefficients

In this case, these coefficients are:

$$K_e := \sqrt{2}$$

$$K_i := \sqrt{2}$$

$$K_p := 0.5$$

4.3. Air gap induction

To approximate the calculation of the induction through the air gap it is necessary to use the expression that better describes the geometry of the rotor armature and the PM properties and position. In this case, the rotor has 10 poles, formed by 10 slots where the PM is mounted, but it does not cover the whole area of the slot, leaving an interior air gap that acts as a flux barrier. It creates a reluctance effect by concentrating the flux through a smaller area. In the next figure it can be seen the rotor configuration with the permanent magnets and the flux barriers created by the air space next to the magnets.
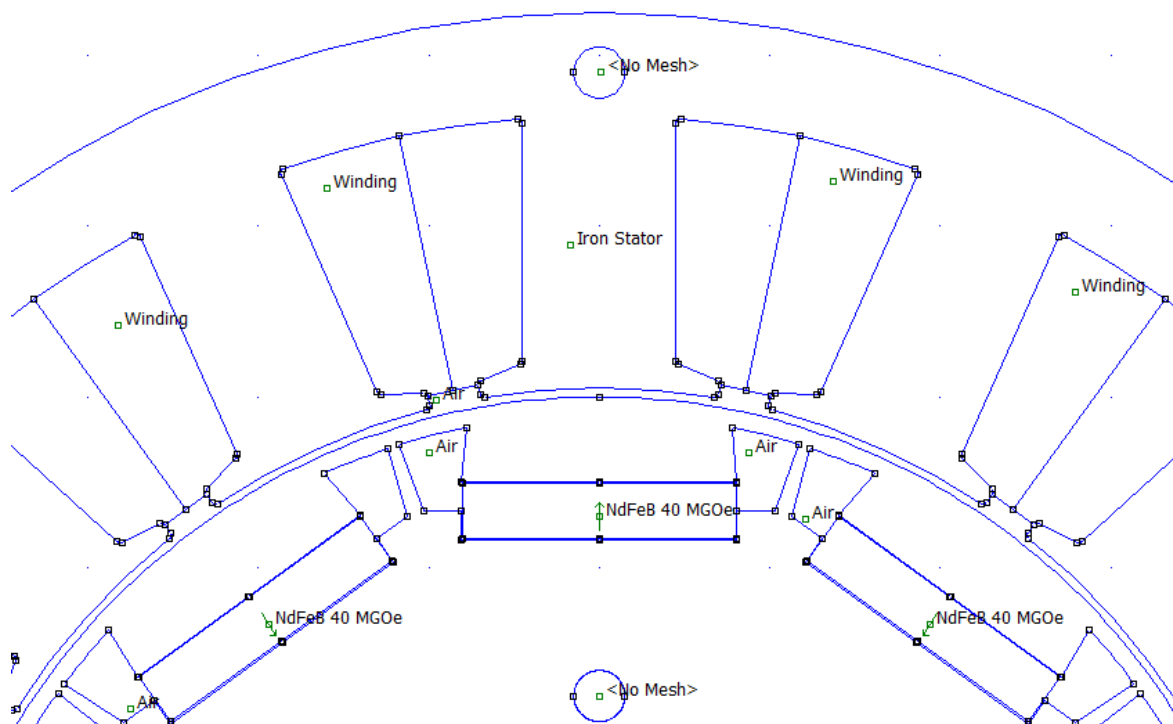
Figure 4.2 – Rotor armature with permanent magnets and air flux barrier

It can be observed in the next figure how this flux barriers affect the flux distribution by concentrating all the flux lines through the magnet.
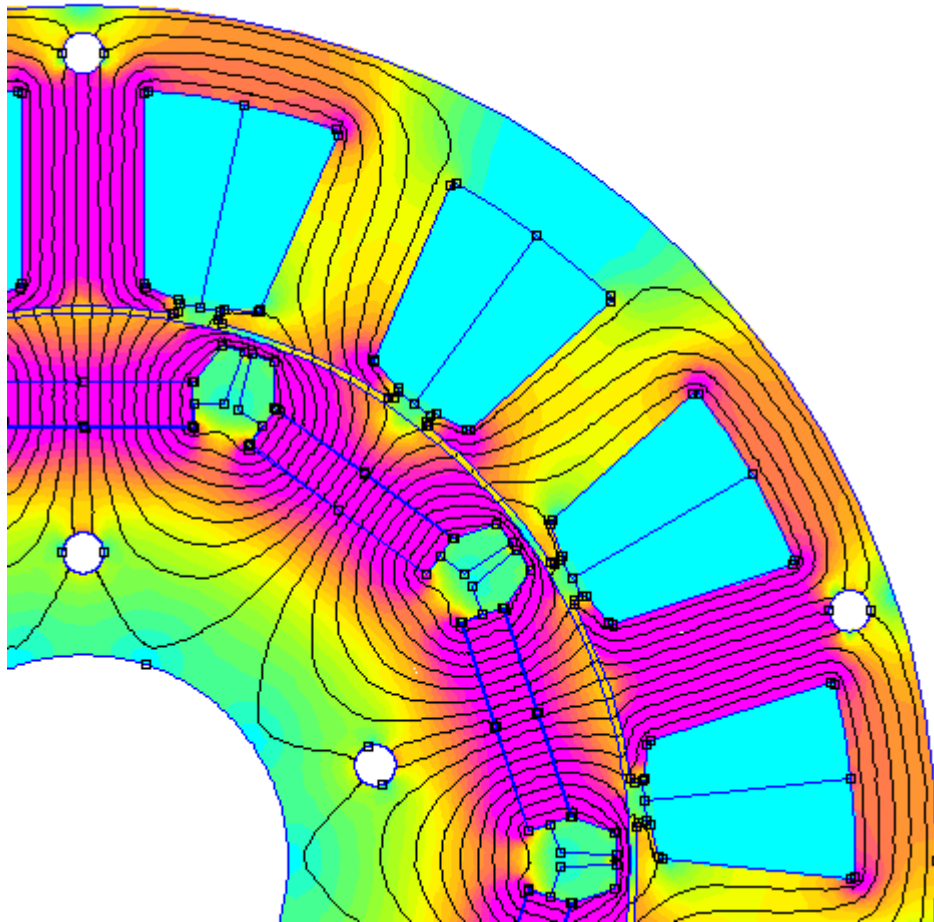
Figure 4.3 – Flux lines concentrated by the effect of the air flux barriers

Understood the induction as the flux that passes through a surface:

$$\Phi = \int_S \vec{B} \cdot d\vec{S}$$

[1.6]

The expression used to relate this rotor geometry and the magnets properties to define the air gap induction is the following:

$$B_e := \frac{B_r - B_{max} \cdot \frac{2 \cdot x}{b_m}}{g_c \cdot \frac{\mu_r}{h_m} + \frac{\Psi \cdot \pi \cdot d_e}{2 \cdot p \cdot b_m}}$$

[1.7]

Where,

- Br: Remain induction of the PM

- Bmax: Max value of the induction in the air gap ≈ 1.7 T

- x: distance from the air slot to the rotor diameter

- hm: thikness of the PM

- bm: width of the PM

- µr: relative permeability of the PM

- de: outer rotor diameter

- ψ and gc: developed on next points

4.3.1. Pole covering factor (ψ)

This factor determines the relationship between the pole step (τp) and the step covered by the width of the PM. Knowing that the pole step is equal to:

$$\tau_p := \frac{\pi \cdot d_e}{2 \cdot p}$$

[1.8]

$$\Psi := \frac{b_m}{\tau_p}$$

[1.9]

Or directly the relationship between angles, obtaining similar results:

$$\Psi := \frac{25}{\dfrac{360}{2 \cdot p}}$$

[1.9.1]

4.3.2. Carter Factor: equivalent air gap (gc)

The Carter factor relates the relative position and geometry of the PM to the outer rotor diameter, obtaining an equivalent air gap width. It can be calculated as:

$$k_c := \frac{\tau_p}{\tau_p - \dfrac{b_g^{\,2}}{5 \cdot g + b_g}}$$

[1.10]

Where,

- g: real air gap

- bg: arc section on the rotor diameter of the space between PM

4.4. Winding

4.4.1. Type of winding

Once the induction on the air gap is calculated, the coils main characteristics can be calculated, taking into account the stator slots and rotor poles. It is useful to calculate the "slots per pole and phase" (q). Knowing the number of slots (Q), the number of pair of poles (p) and the number of phases of the supply system (m):

$$q := \frac{Q}{2 \cdot p \cdot m}$$

[1.11]

In this case, is needed to build a concentrated winding system of two layers.

With the software "Koil" it can be confirmed the implementation of the concentrated winding and the winding factor, which because of this distribution affects the electromotive force that the coils can generate. In the following images can be seen the winding system calculated with "Koil": Concentrated double layer winding system.
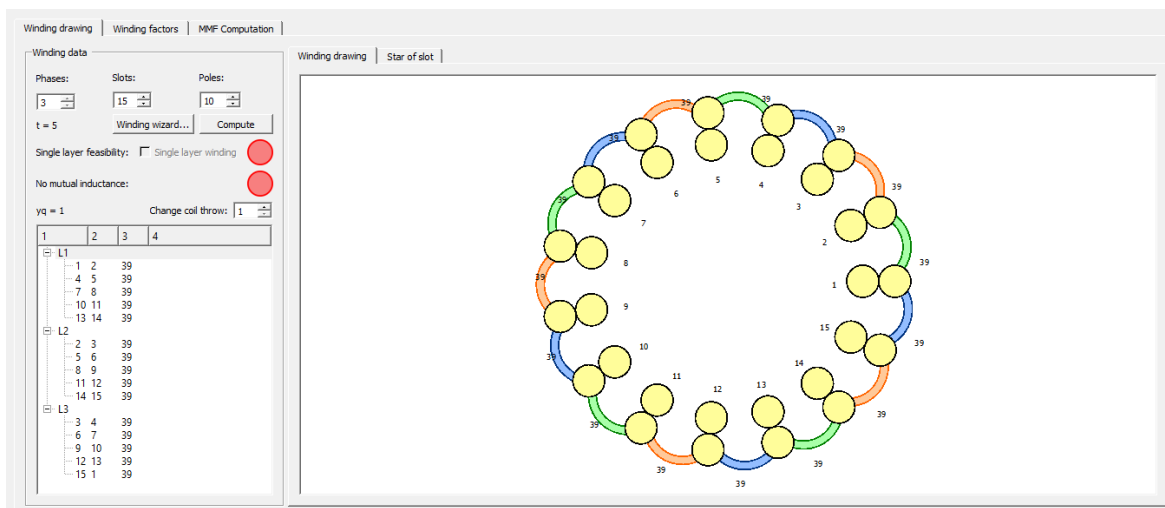
Figure 4.4 – Concentrated winding generated with software "Koil"
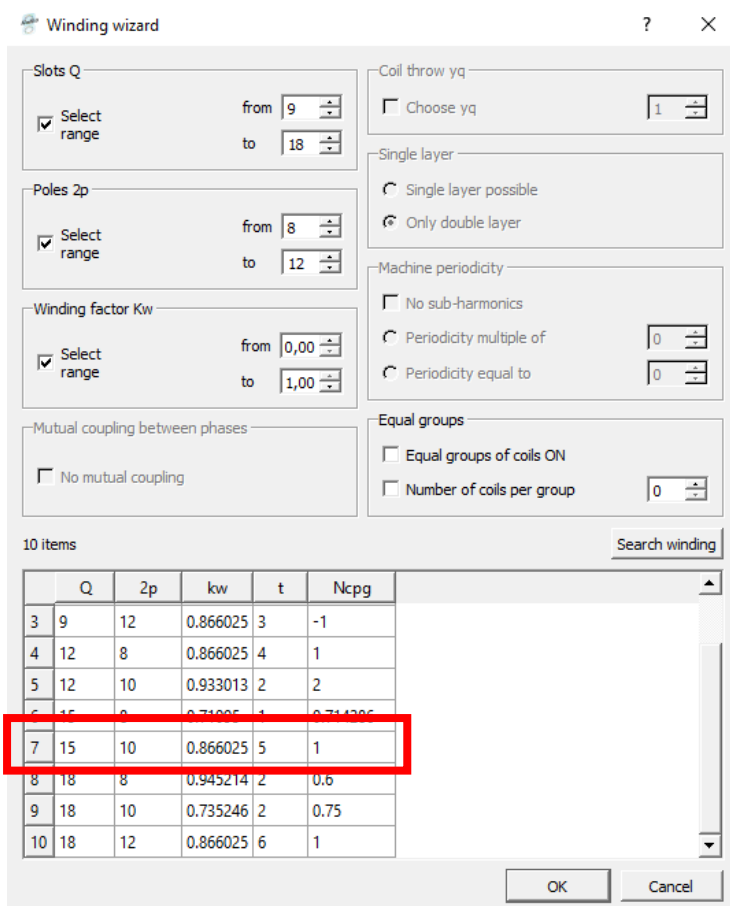
Figure 4.5 – Winding factor(kw) for 15 slots and 10 poles machine (software "Koil")

UNIVERSITAT POLITÈCNICA DE CATALUNYA
BARCELONATECH
Escola d'Enginyeria de Barcelona Est

4.4.2. Number of turns per phase

The number of turns per phase will determine the characteristics of the machine. They are calculated to achieve the nominal conditions of the motor.

The electromotive force that the phase coil needs to transmit to the rotor is approximate as a 90% of the phase voltage, resulting E ≈120 V. It depends also from the flux created by the induction in the airgap, where L is the longitude of the machine:

$$\Phi := \frac{2}{\pi} \cdot B_e \cdot \tau_p \cdot L$$

[1.12]

Knowing all the parameters involved in the equation, the number of turns per phase results:

$$N_f := \frac{E}{\frac{2\,\pi}{\sqrt{2}} \cdot \xi_b \cdot \Phi \cdot fs}$$

[1.13]

Note that the number of turns is affected by the winding factor (ξb) and the synchronous frequency.

4.4.3. Conductors bore diameter

Once the number of turns per phase is calculated, the conductors diameter needs to be determined, according to the current density and the available space of the stator slot.

Knowing the number of turns per phase, the total number of conductors (Zt) can be calculated in order to determine the resulting current layer of the windings, and confirm if this value is between the normalized parameters.

$$Z_t := 2 \cdot m \cdot N_f$$

[1.14]

With the nominal current of the machine and the outer diameter of the stator, the current layer is:

UNIVERSITAT POLITÈCNICA DE CATALUNYA
BARCELONA**TECH**

Escola d'Enginyeria de Barcelona Est

$$As := \frac{Z_t \cdot In}{\pi \cdot D_e}$$

[1.15]

The area of the conductor can be calculated as the relationship between the nominal current of the machine and the current density (Δ), which normal values are between 2 and 8 A/mm^2.

$$S_c := \frac{In}{\Delta}$$

[1.16]

Knowing the area of the conductor, the conductor bore diameter can be calculated as:

$$d_c := \sqrt{\frac{4 \cdot S_c}{\pi \cdot aa}}$$

[1.17]

Where, "aa" is the number of strands, or parallel wires forming one conductor. By increasing the number of strands, the bore diameter of the conductor will significantly decrease.

The diameter chosen is the immediately superior normalized diameter to the result obtained.

It is necessary at this point, to check if the calculated coils will entirely fit in the slot. The occupied surface (Soc) of the coil is calculated with the number of conductors per slot (Zr).

$$Z_r := \frac{Z_t}{Q}$$

[1.18]

$$S_{oc} := aa \cdot Z_r \cdot \pi \cdot \frac{d_c^2}{4}$$

[1.19]

Knowing the occupied area of the conductors and calculating the area of the slot (Sr), it can be confirmed if the coils fit in the slot:

$$F_{oc} := \frac{S_{oc}}{S_r}$$

[1.20]

UNIVERSITAT POLITÈCNICA DE CATALUNYA
BARCELONATECH
Escola d'Enginyeria de Barcelona Est

The fill factor (Foc) calculated cannot be bigger than 0, 4. This value takes into account the thickness of the wires insulation and the film insulation. It is important to achieve a number close to 0,4 in order to have a better efficiency by filling the entire available area of wires.

4.5. Inductances

The calculations of the main inductances in PMSMs have to be done according the geometry and position of the PM on the rotor. For a Non-Salient poles machine, the airgap is constant, so the inductance in the d-axis and the inductance on the q-axis are the same: the magnetizing inductance of the machine.

But in Salient pole machines, the airgap cannot be consider as constant, so the inductances on the d-axis and the q-axis are different. Considering that the magnetic permeability in the PM is similar to the vacuum magnetic permeability, the q-axis inductance is bigger than the d-axis inductance: Lq > Ld.
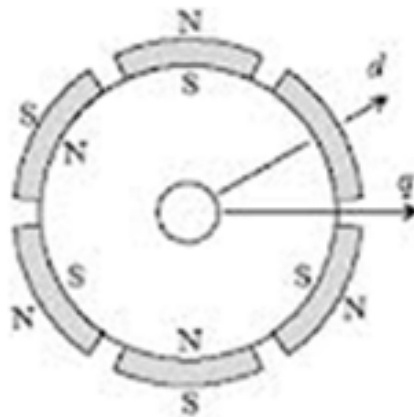
Figure 4.6 – Salient pole machine d- axis and q-axis

The configuration of the rotor considered in this work is a buried interior permanent magnet with tangential magnetization direction. It can be considered as a Salient pole machine, so inductances in d and q axis are different, being Lq bigger than Ld.
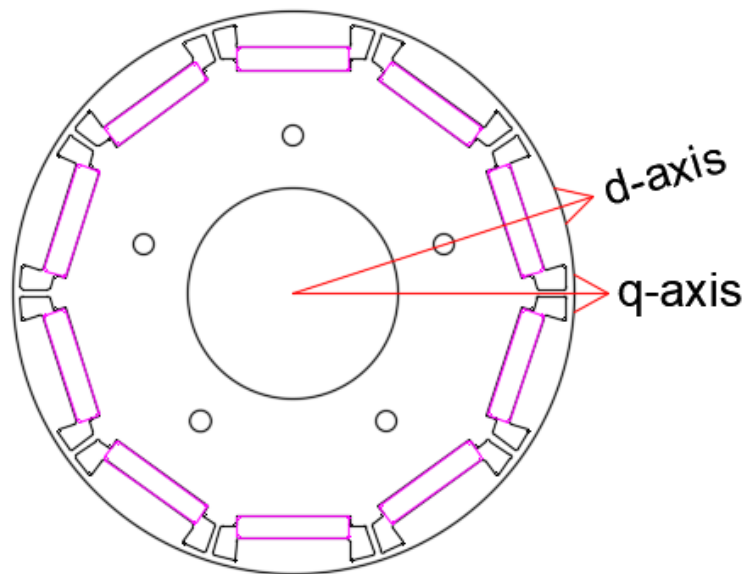
Figure 4.7 – Designed rotor: Considered a Salient pole machine with different inductances in d- axis and q-axis

4.5.1.   Main inductances

To estimate both inductances of the machine, the magnetizing inductance needs to be calculated, as if it were a Non Salient poles machine, and then, the Ld and Lq inductances are going to be determined with a kd and kq factors as follow:

$$L_m := \frac{\mu_0}{\pi} \cdot m \cdot \frac{D_e \cdot L}{g_c} \cdot \left(\frac{N_f \cdot \xi_b}{p}\right)^2$$

[1.21]

Where μ0 is the vacuum magnetic permeability

$$L_{mq} := L_m \cdot k_q$$

$$L_{md} := L_m \cdot k_d$$

[1.22]

Being the expressions of those factors for the considered rotor geometry:

$$k_q := \frac{(\Psi \cdot \pi - \sin(\Psi \cdot \pi))}{\pi}$$

[1.23]

UNIVERSITAT POLITÈCNICA DE CATALUNYA
BARCELONATECH
Escola d'Enginyeria de Barcelona Est

$$k_d := \left[\frac{\left(\sin\left(\frac{\Psi \cdot \pi}{2} \right) \right)^2}{\frac{\Psi \cdot \pi}{2} + p \cdot g_c \cdot \mu_r \cdot \frac{b_m}{h_m \cdot D_i}} \right] \cdot \frac{4}{\pi} - k_q$$

[1.24]

4.5.2. Stray inductance

In the machines are different types of inductances but not all of them participating directly of the electromechanical conversion of energy. One of them is the stray inductance. It is created by the flux lines that do not pass through the air gap, instead they close themselves through the slot. On figure 4.7 can be seen the flux lines and a diagram of many important distances to calculate this stray inductance. It depends directly of the slot geometry. In this case, the considered slot is from the shown type.
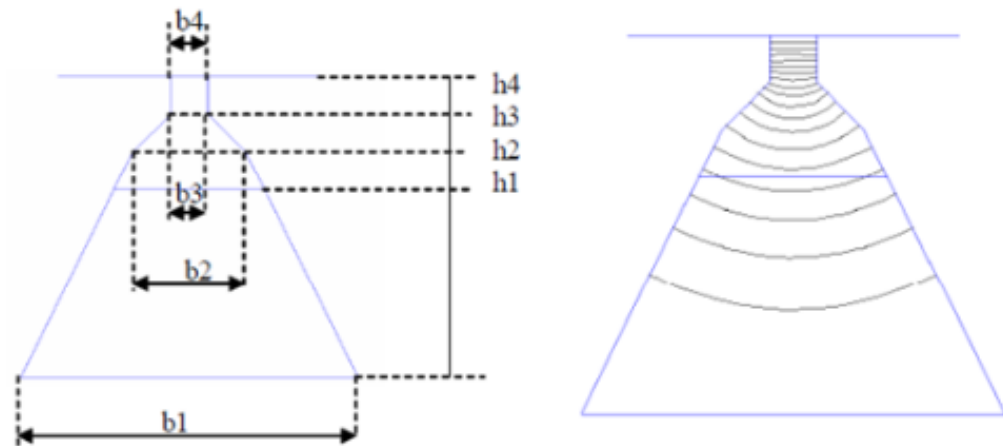
Figure 4.7 – Distances to calculate the stray inductance and flux lines of stray inductance

The expression used to calculate the stray inductance is:

$$L_r := \mu_0 \cdot N^2 \cdot L \left(\frac{2 \cdot h_1}{3 \cdot (b_1 + b_2)} + \frac{(h_2 - h_1)}{b_2} + \frac{(h_3 - h_2)}{b_2 - b_4} \cdot \ln\left(\frac{b_2}{b_4} \right) + \frac{(h_4 - h_3)}{b_4} \right)$$

[1.25]

Adding this stray inductance to the magnetizing inductance and multiplying with the kd and kq factors will result in the total Ld and Lq inductances.

There are other types of inductances not taking part in the electromechanical conversion of energy, such as the differential inductance created by the harmonics of the magnetomotive force in the air gap. This predesign study takes into account only the fundamental harmonic of the magnetomotive force. So it will not be studied, along with the stray inductance produced on the head coil, because the next steps of the design will include these concepts.

4.6. Losses and thermal calculations

The thermal calculations are very important in order to design this kind of machine. Many of the designed prototypes could achieve the desired characteristics, but cannot work properly because of the temperatures generated. The heat could be ventilated with fins or with a fan. The procedure to calculate the heating of the machine starts with the calculations of the losses in the machine, because they are the only responsible for the heating.

The Joule losses generated in the coils can be calculated as:

$$P_j := 3 \cdot R \cdot I^2$$

[1.25]

And the iron losses estimated as:

$$P_{fe} := \frac{1}{3} \cdot P_j$$

[1.26]

The phase resistant needs to be determine with the copper resistivity at 100°C, the number of turns per phase, and the longitude and area of the conductors, resulting in the following expression:

$$R := N_f \cdot \rho_{Cu100} \cdot \frac{l_{esp}}{S_c}$$

[1.27]

Knowing the losses of the machine, the maximum heating (θ) needs to be determine with the equation:

$$\Theta := \frac{Losses}{K_v \cdot S_v}$$

[1.28]

UNIVERSITAT POLITÈCNICA DE CATALUNYA
BARCELONATECH
Escola d'Enginyeria de Barcelona Est

Where, Sv is the ventilation surface, taking into account the outer diameter and the longitude of the casing, and Kv is the ventilation coefficient of the machine. Setting the maximum heating to the normalized value, it can be obtain as follows:

$$K_v := 1.32 \cdot \sqrt[4]{\frac{1000 \cdot \Theta_{max}}{D_{ext} \cdot 10^3}}$$

[1.28]

If the heat value is bigger than the maximum set, appears the need to improve the ventilation. In order to evacuate more heat, fins are added to the casing. The expressions used to calculate the new maximum heat value are the same as before, but with fins, the ventilation surface increase considerably. If the new and bigger ventilation surface is applied to expression [1.28], the maximum heat will decrease.

4.7. Analytical results

All the calculations and results obtained can be seen on the Annex A. On the next table are resumed the main result obtained. These results approximate the end characteristics of the motor.

Analytical Results at rated speed 1500 rpm	
Torque [N.m]	14,006
Power [W]	2200
Phase Voltage[V]	120
Phase Current [A]	7,55
Efficiency[%]	91,4
Power Factor	0,8
Copper Loss [W]	149,47
Iron Loss [W]	49,82
Wire Current Density [A/m$^{2]}$]	7,51E+06
Ld [H]	7,00E-03
Lq [H]	0,009
Number of turns per coil	35

Table 4.2 – Analytical results

UNIVERSITAT POLITÈCNICA DE CATALUNYA
BARCELONA**TECH**
Escola d'Enginyeria de Barcelona Est

UNIVERSITAT POLITÈCNICA DE CATALUNYA
BARCELONATECH
Escola d'Enginyeria de Barcelona Est

5. JMAG Design

The free license software JMAG allows to design a motor, confirming and adjusting the parameters obtained with the analytical calculations. It makes a quick simulation with the parameters introduced obtaining the characteristics of the design. It takes into account many more parameters than the ones calculated analytically.

The methodology followed was to entry the analytical results of the parameters and adjust some of the parameters, such as the number of turns and the wire diameter in order to achieve as result for the nominal phase voltage around 120V, at least the nominal torque and the nominal power.

5.1. Data entry

5.1.1. Dimensions

To introduce the main dimension parameters and create the motor diagram, the type of motor, stator armature and rotor armature have to be chosen. Dimensions have been introduced as follows:

Figure 5.1– JMAG Motor dimensions

Then, the motor diagram is created, where it can be seen the number of slots and poles:
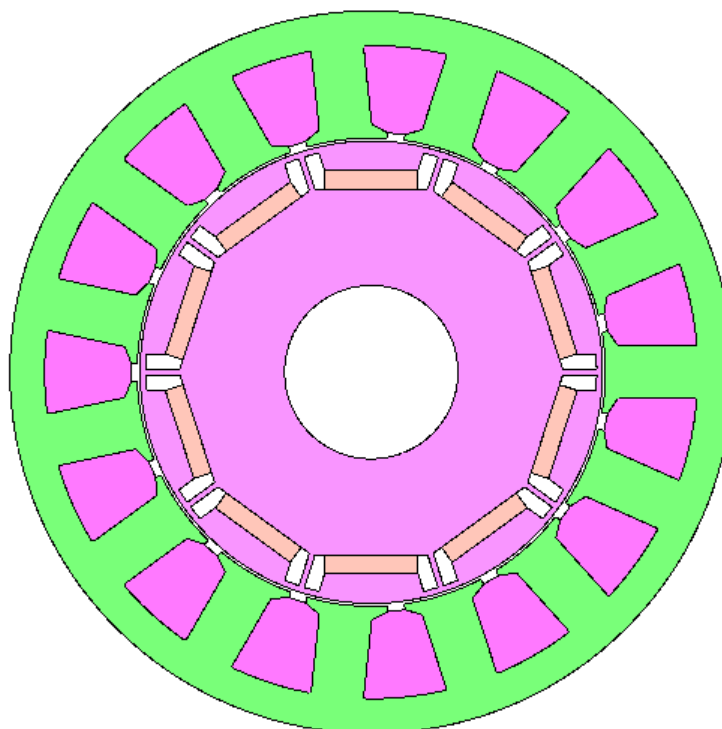
Figure 5.2– JMAG Motor diagram

The materials are defined. In this case the steel M470 50A is chosen for stator and rotor structure. It`s shows the characteristic B-H curve. Copper has been chosen for the coils.
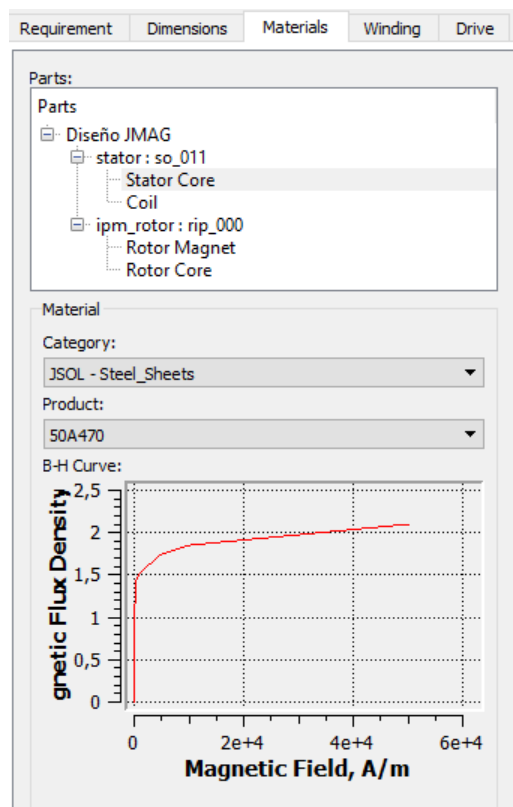
Figure 5.3– JMAG Materials

5.1.2. Winding

To create the coils, the parameters shown in the next figure have to be introduced. The number of turns refers to the number of turns per coil, which can be calculated from the next expression, where "Nf" is the number of turns per phase, and the number 5 refers to the number of series coils of one phase:

$$N_b := \frac{N_f}{5}$$

[2.1]

The slot fill factor has to be less than 75%, but as closer as possible to fill the slot as much as possible. Also by changing the wire diameter, a considerable reduction of the losses is achieved.

UNIVERSITAT POLITÈCNICA DE CATALUNYA
BARCELONATECH
UPC Escola d'Enginyeria de Barcelona Est
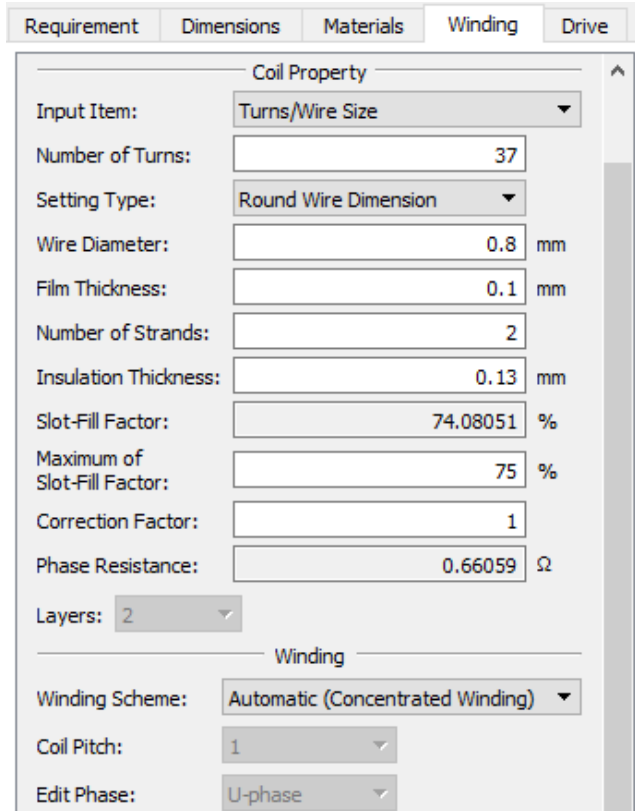
Figure 5.4– JMAG Winding parameters

It can be also seen the winding diagram and the slot diagram, where it is described how the winding is coiled.
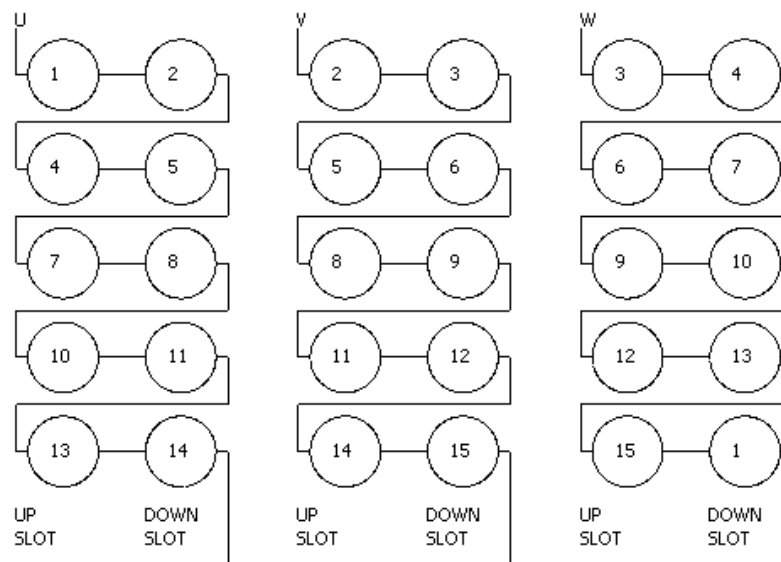
Figure 5.5– JMAG Winding diagram
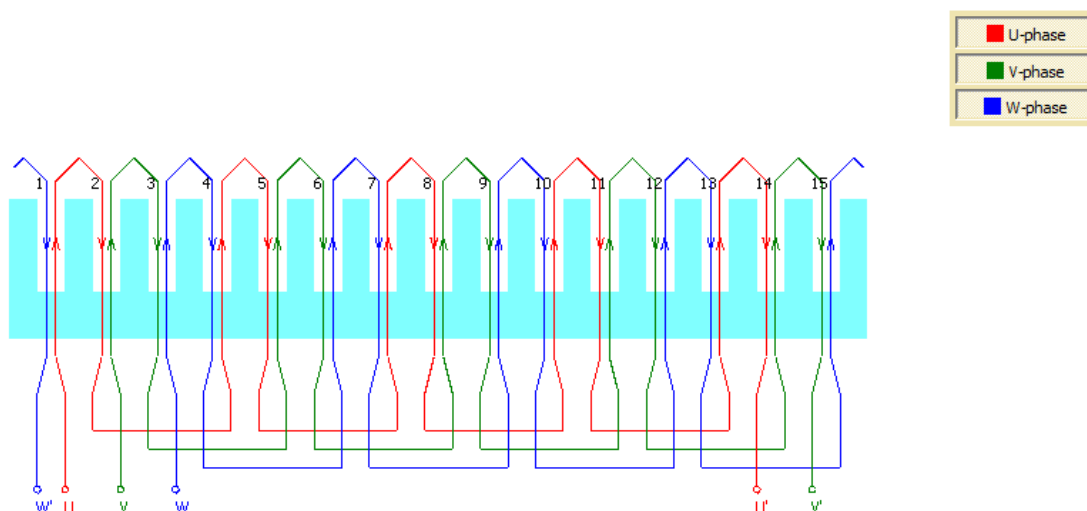
Figure 5.6– JMAG Slot diagram

5.1.3. Drive

Finally the power supply parameters have to be introduced. The motor is going to be calculated for a voltage sinusoidal supply system. The line voltage peak as RMS Line Voltage multiplied by "sqrt(2)". And the maximum line current can be calculated as the nominal current multiplied by "sqrt(2)".
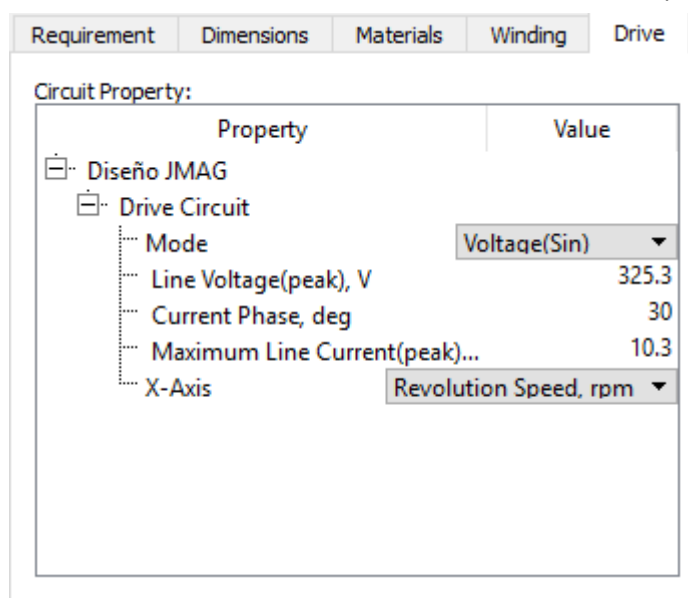
Figure 5.6– JMAG Drive parameter input

5.2. JMAG Results

After the calculations, JMAG delivers the results obtained. All the results can be seen on the Annex B. On the next figures can be observed the results obtained, which are resumed on the following table:

JMAG Results at rated speed 1500 rpm	
Torque [N.m]	14,55
Power [W]	2285
Phase Voltage[V]	115,9
Phase Current [A]	7,283
Efficiency[%]	94,41
Power Factor	0,9554
Copper Loss [W]	105,1
Iron Loss [W]	29,85
Wire Current Density [A/m$^{2]}$	7,25E+06
Ld [H]	9,63E-03
Lq [H]	0,01796
Number of turns per coil	37

Table 5.1– JMAG main results

6. Magnetic Analysis with Finite Elements Magnetics Method

After the initial calculations and the adjustments performed on JMAG, the motor is going to be analyzed with the free software FEMM in order to confirm the characteristics and operation points. Through simple LUA scripts to perform the simulations and after data process in Excels calculations sheets, the characteristics and behavior of the machine is going to be determined.

6.1. Armatures draws and material definition

The start point is the draw of the geometry of the armatures and magnets of the machine. To simplify this process, this draw was done directly in AutoCAD from the existing armatures draws. After that it can be easily import to FEMM as a "dxf" file.

Figure 6.1– AutoCAD Draw

UNIVERSITAT POLITÈCNICA DE CATALUNYA
BARCELONATECH
Escola d'Enginyeria de Barcelona Est
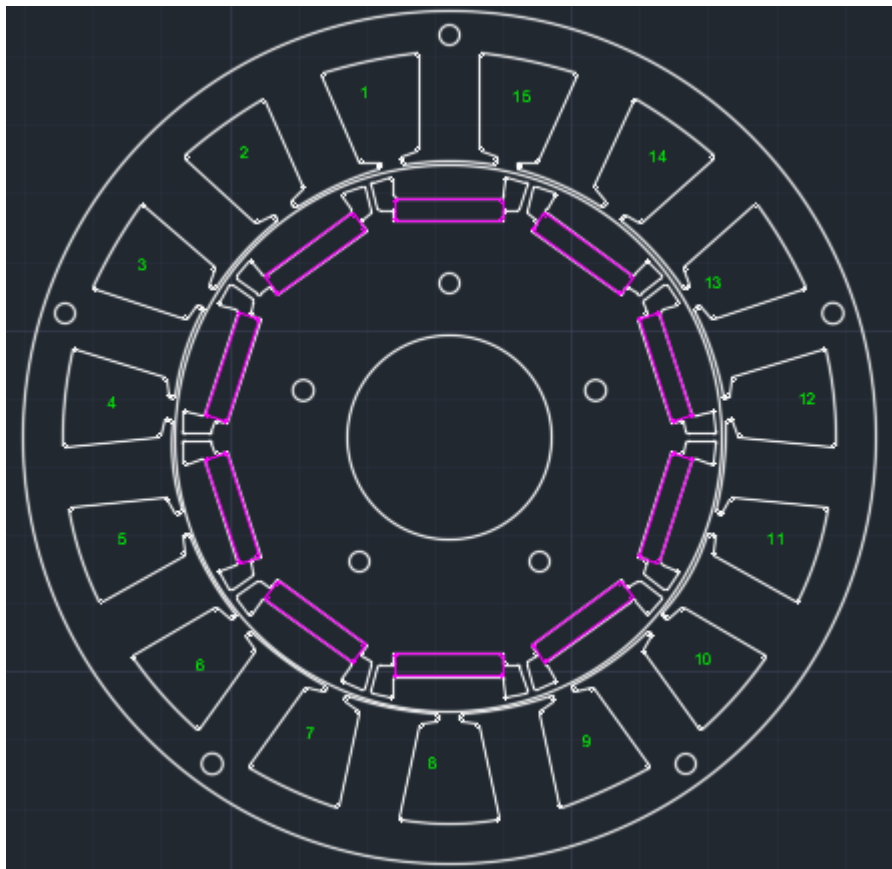
After importing the draw to FEMM, all the materials were defined and assigned to the corresponding area of the machine, defining also the number of turns per coil, the magnetizing direction of the PM and the boundary conditions to the outer diameter of the stator:
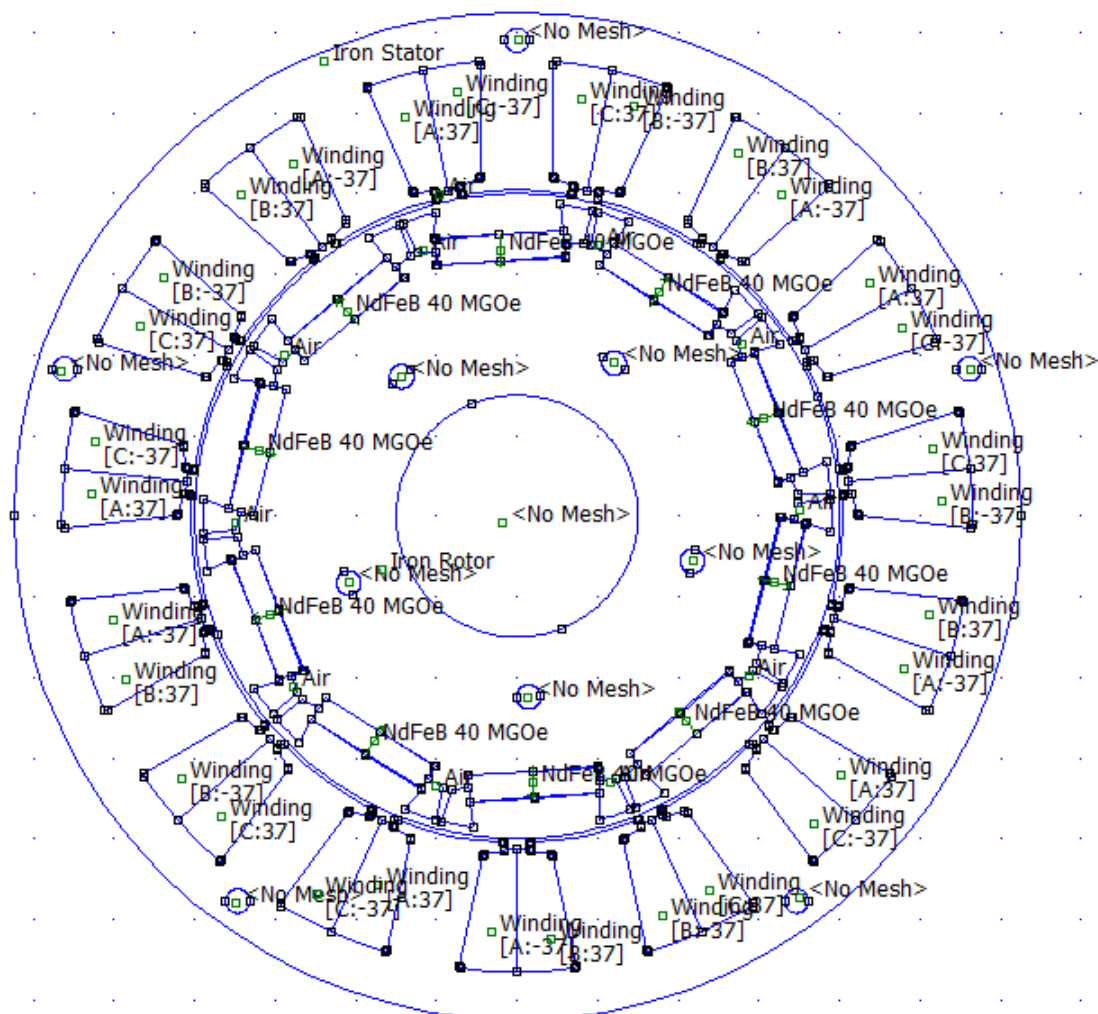
Figure 6.2– FEMM Draw and materials definition

6.2. Cogging torque optimization

Before starting the simulations that will determine the characteristics and operation points of the machine, the cogging torque is going to be analyzed and according to the results, the geometry of the rotor slightly changed.

The cogging torque is generated due to the interaction of the PM and the stator teeth's. It is a not desired effect of the magnets and affects negatively the functioning of the machine, generating noise and damaging vibrations.

UNIVERSITAT POLITÈCNICA DE CATALUNYA
BARCELONATECH
Escola d'Enginyeria de Barcelona Est

Years ago, after the fact was deeply studied, and with empirical verifications, it could be demonstrated, that one of the factors that could reduce the cogging torque was to have in the rotor geometry a certain angle for the opening of the free space slot. There are other methods as well to reduce the cogging torque, but not applied in this work.

The objective of the simulation is to reduce the cogging torque by changing the angle α until a minimum cogging torque value is found.
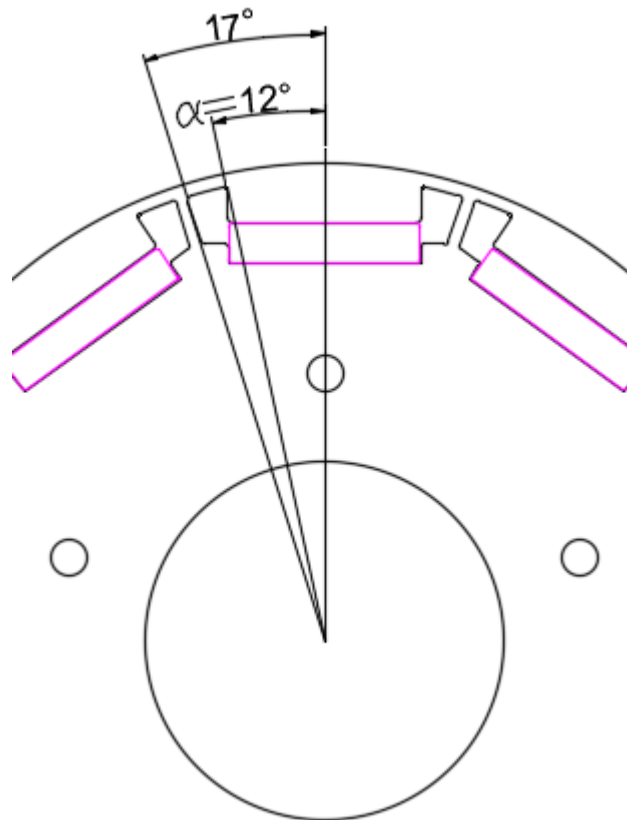
Figure 6.3– Angle α can be change in order to reduce the cogging torque

The expected result after simulating between angles from 10 to 15 degrees is to find the angle where the torque is minimum. Different geometries have different angle results. The next figure illustrates the expected behavior of the torque in relationship with angle α.
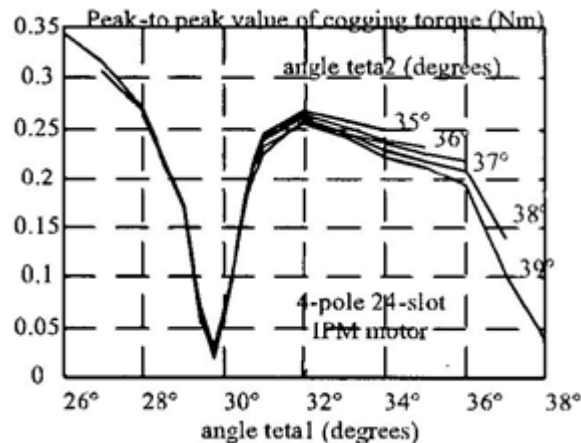
Figure 6.4– By changing the angle can be reduced the cogging torque

6.2.1. Simulation cogging torque

A LUA script was written in order to study the cogging torque generated by the PM for each angle between 10 and 15 degrees. The iteration process is based in drawing the rotor geometry with a certain angle, also with a LUA script, and then perform the simulation to determine the cogging torque in each position for the mechanical angle of a pair of poles. Then the rotor is erased and drawn again with the next angle and simulated again.

The entire LUA script used for the draw, material definition and simulation can be found on Annex C. Note that for this simulation, the current is 0 A. Only the magnets effects are analyzed. The cogging torque simulation LUA script used is:

```lua
--COGGING SIMULATION
  periode=360/10;
  step=periode/20;

  for deg=0, 2*periode, step do

    mi_analyze(1);
    mi_loadsolution();

    --cogging torque calculation routine
    mo_groupselectblock(99)
    cog=mo_blockintegral(22)  --(Steady-state weighted stress tensor
torque)
    mo_clearblock()

    --Motor rotation
    mi_seteditmode("group")
```

```
mi_selectgroup(99)
mi_moverotate(0,0,step)

--store on file
handle=openfile("Cogging RESULTS.txt","a")
write(handle,deg,"  ",cog,"  ","\n")
closefile(handle)
mo_close()
end
```

6.2.2. Results

The cogging torque was analyzed for 40 points in a period of one pole and for 6 different α angles. The results obtained were then processed with Excel. In the next graph, the maximum cogging torque value of each angle is shown.
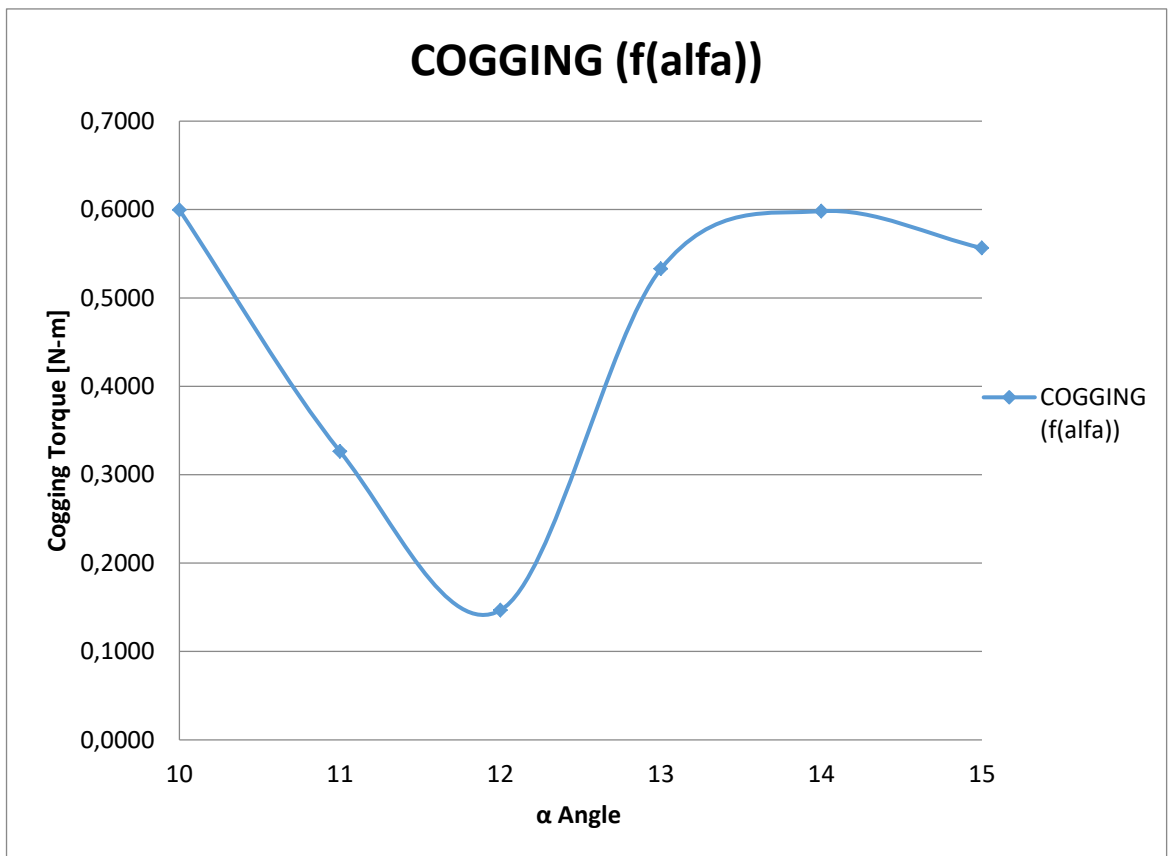
Figure 6.5– Cogging torque in front of angle α

A second simulation was performed in order to achieve more accurate results. Knowing that the minimum torque was around 12 degrees, the whole process was done again with angles between 11 and 13 degrees, obtaining following results.
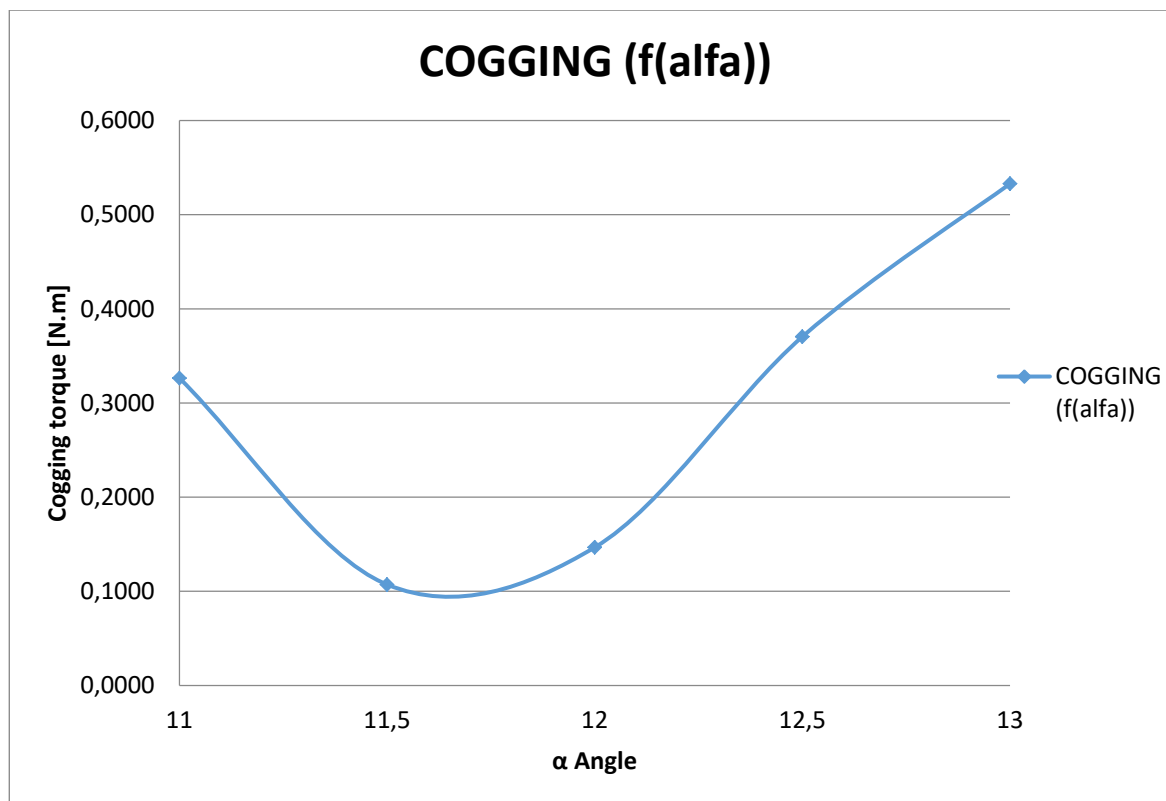
Figure 6.6– Cogging torque in front of angle α (Accurate)

After the results obtained, the rotor geometry is slightly changed in order to optimize the motor functioning by reducing the cogging torque.

Finally the cogging torque results with the selected α angle= 11.5° are shown on the graph. The maximum cogging torque peak is 0,1 N.m, which represent less than 1% of the nominal torque of the machine.
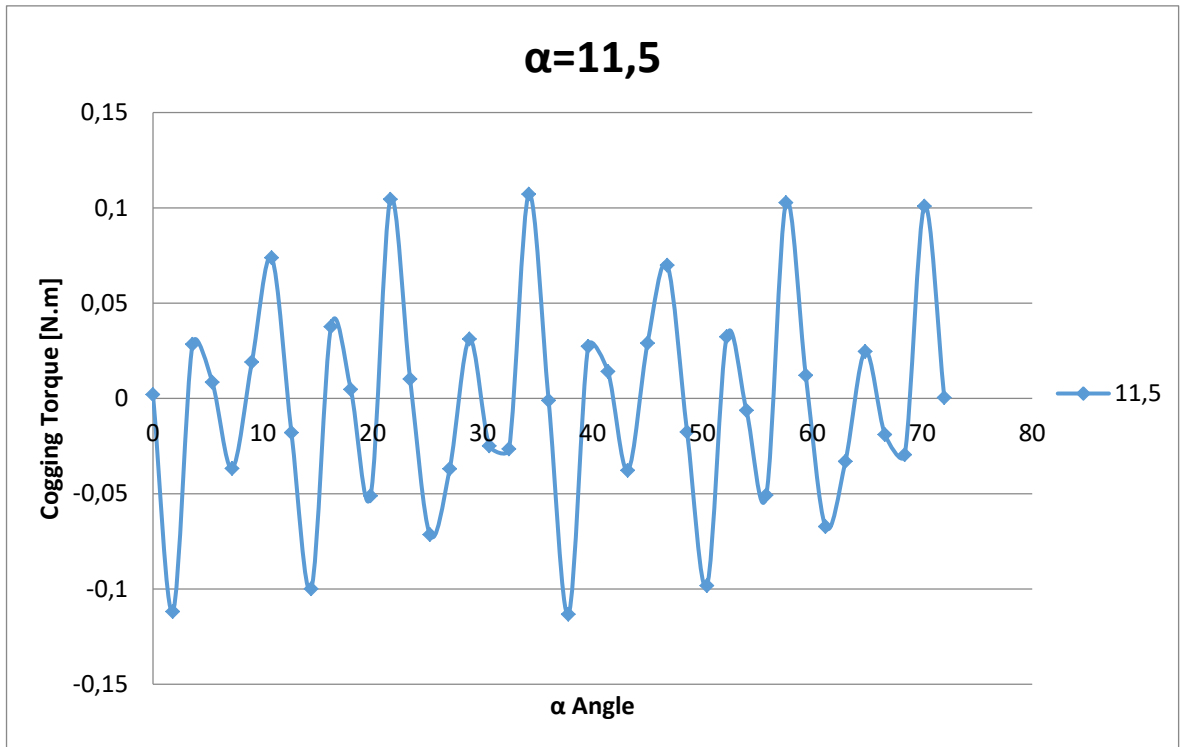
Figure 6.7– Cogging torque obtained with optimized α angle

6.3. No Load Analysis: CEMF determination

Once the rotor geometry is defined and the cogging torque verified, the no load simulation can be performed. The back electromotive force or counter electromotive force, known as "CEMF" is produced by the permanent magnets.

6.3.1. Simulation

Again the current through the coils is 0 A, in order to determine the flux created by the PM and the electro motive force (EMF) induced.

The LUA script used is the following:

```
--NO LOAD Simulation
```

UNIVERSITAT POLITÈCNICA DE CATALUNYA
BARCELONATECH
Escola d'Enginyeria de Barcelona Est

```
mi_modifycircprop("A",1,0); --0 A Current
mi_modifycircprop("B",1,0);
mi_modifycircprop("C",1,0);
showconsole()
data={};
steps=40;
p=5;

--mechanical degrees increase
delta=(360/p)/steps;
for k=1,(steps+1) do
print((k-1).."/"..steps);
mi_analyze(1);
mi_loadsolution();
data[k]={};

--position in mechanical and electrical degrees
data[k][1]=(k-1)*delta;
data[k][2]=p*data[k][1];

--Data from circuits
ca,va,fa=mo_getcircuitproperties("A");
cb,vb,fb=mo_getcircuitproperties("B");
cc,vc,fc=mo_getcircuitproperties("C");
data[k][3]=fa;
data[k][4]=fb;
data[k][5]=fc;

--Motor rotation
mi_selectgroup(99);
mi_moverotate(0,0,delta,4);
mi_clearselected();
end

--store in file
fp=openfile("Resultados de flujo.txt","w");
for k=1,(steps+1) do
write(fp,data[k][1]," ",data[k][2]," ",data[k][3]," ",data[k][4],"
",data[k][5], "\n")
end
closefile(fp);
```

To calculate the CEMF the fluxes can be derivate respect its mechanical position and multiplied with its speed, as describes the followings expressions:

$$e_a := \frac{\phi_2 - \phi_1}{\theta_2 - \theta_1} \cdot \omega$$

[6.1]

UNIVERSITAT POLITÈCNICA DE CATALUNYA
BARCELONA**TECH**
Escola d'Enginyeria de Barcelona Est

$$\omega := \frac{2 \cdot \pi}{60} \cdot N_n$$

[6.2]

6.3.2.   Results

The results are resumed in next two graphs. The RMS CEMF calculated is 98,13 V.
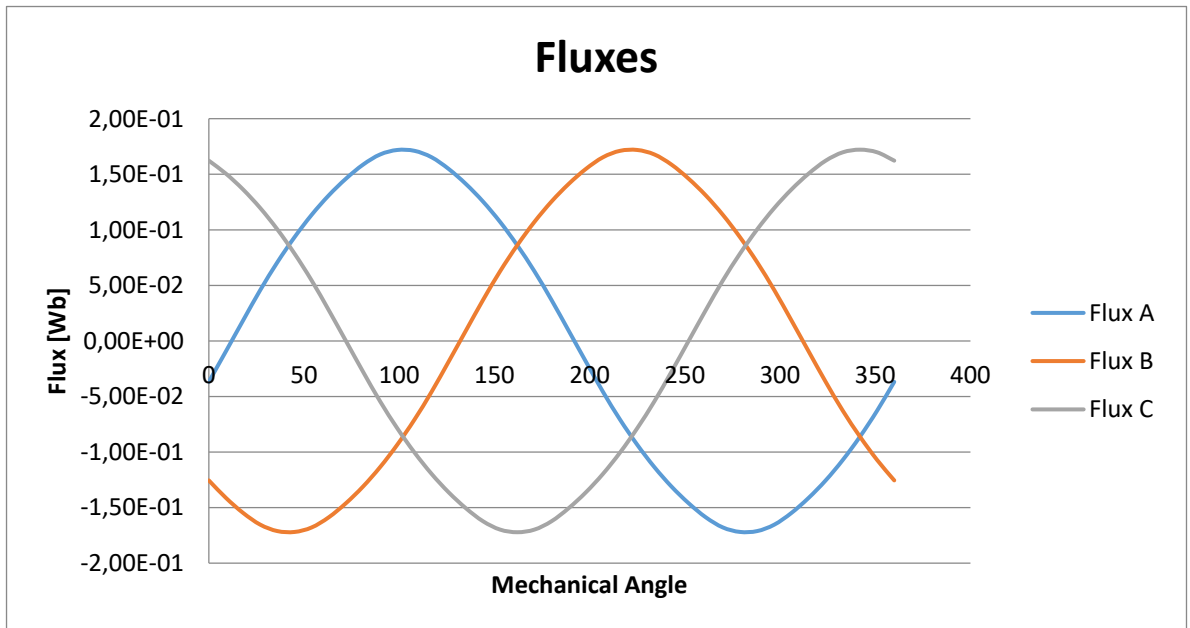
Figure 6.8– Phase fluxes due to the magnets
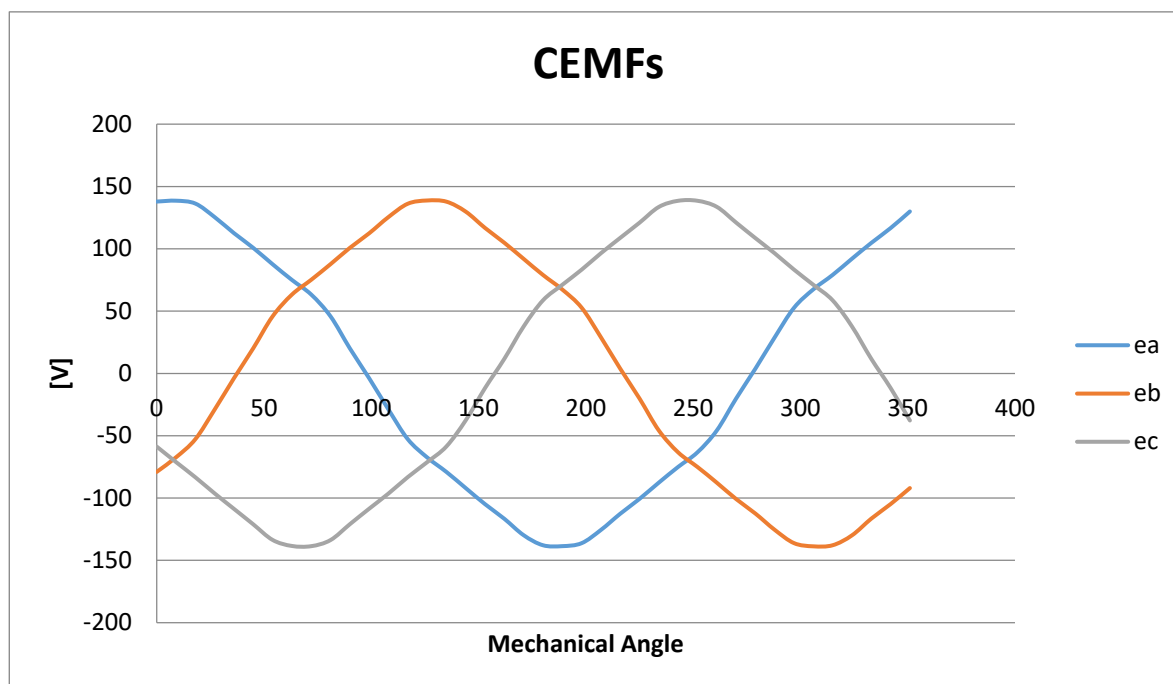
Figure 6.9– Phase CEMFs

6.4. Load Analysis: Delta Torque

The delta torque is the one generated by the same nominal current on each position of the rotor. It's not constant, because the current is not changing in time.

6.4.1. Simulation

For this analysis the current of the phases is the nominal current of the machine. The correct format to introduce the current in FEMM is the following:

In*sqrt(2)

In*sqrt(2)*(-0.5-I*(sqrt(3)/2))

In*sqrt(2)*(-0.5+I*(sqrt(3)/2))

FEMM works with the peak values of the current and in a three-phase balanced system, when phase A is at his positive maximum, phases B and C crosses their half negative value.

UNIVERSITAT POLITÈCNICA DE CATALUNYA
BARCELONATECH
Escola d'Enginyeria de Barcelona Est

Then the torque routine is performed for each position with these current values. The LUA script used is written next:

```lua
--Delta Torque Simulation
p=5
periode=360/p
step=periode/20

for deg=0, 2*periode, step do

  mi_analyze(1)
  mi_loadsolution()

  --torque calculation routine
  mo_groupselectblock(99)
  MI=mo_blockintegral(22)--Steady-state weighted stress tensor torque
  mo_clearblock()

  --Motor rotation
  mi_selectgroup(99)
  mi_moverotate(0,0,step)

  --store on file
  handle=openfile("Resultados Par delta.txt","a")
  write(handle,deg,"    ",MI,"\n")
  closefile(handle)
  mo_close()
end
```

6.4.2. Results

After the results are obtained, it is necessary to rotate the rotor to the position where the torque has its maximum value, position known as MTPA: "Maximum Torque Per Ampere".

The results obtain are shown on next graph. The nominal torque is achieved with nominal current. The whole result table can be seen in Annex C.

UNIVERSITAT POLITÈCNICA DE CATALUNYA
BARCELONATECH
Escola d'Enginyeria de Barcelona Est
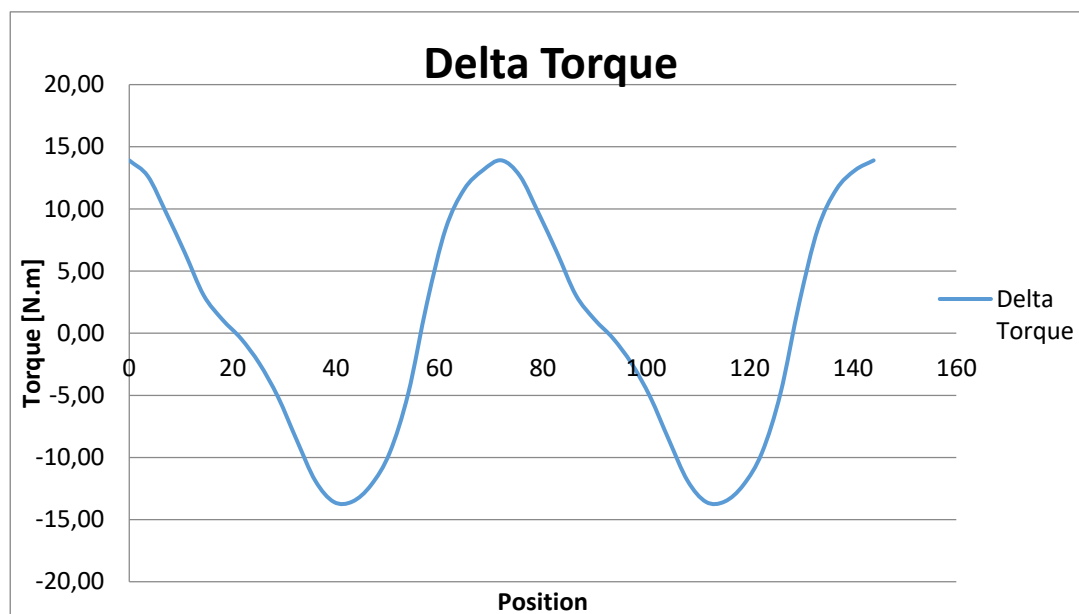
Figure 6.10– Delta Torque. With nominal current reaches the nominal torque

6.5. Load Analysis: Rotating Torque

The rotating torque is the one generated when the machine rotates at nominal speed, fed by his nominal current.

6.5.1. Simulation

In order to achieve this load analysis of the machine when it rotates at the rated speed, it is necessary to create a supply system variable in time. Machine is fed by its nominal current. With the next LUA script it is possible to simulate the rotating machine and its variable in time supply system.

```
--Load Simulation
pi=3.1415926
p=5
periode=360/p
step=periode/20
Imax=7.283*sqrt(2)
alfa=0
```

UNIVERSITAT POLITÈCNICA DE CATALUNYA
BARCELONATECH
Escola d'Enginyeria de Barcelona Est

```
for deg=0, 2*periode, step do

  --time variable currents
  Ia=Imax*cos(alfa*pi/180)
  Ib=Imax*cos(alfa*pi/180-2*pi/3)
  Ic=Imax*cos(alfa*pi/180+2*pi/3)
  mi_modifycircprop("A",1,Ia);
  mi_modifycircprop("B",1,Ib);
  mi_modifycircprop("C",1,Ic);

  mi_analyze(1)
  mi_loadsolution()

  --torque calculation routine
  mo_groupselectblock(99)
  MI=mo_blockintegral(22)--Steady-state weighted stress tensor torque
  mo_clearblock()

  --Circuits properties
  ia,va,fa=mo_getcircuitproperties("A")
  ib,vb,fb=mo_getcircuitproperties("B")
  ic,vc,fc=mo_getcircuitproperties("C")
end

--Motor rotation
  mi_seteditmode("group")
  mi_selectgroup(99)
  mi_moverotate(0,0,step)
  alfa=alfa+p*step

  --store on file
  handle=openfile("Resultados Par girando.txt","a")
  write(handle, deg,"  ", MI,"  ", Ia," ", Ib," ", Ic,", ",\n")
  closefile(handle)
  mo_close()

end
```

6.5.2. Results

The results obtained can be seen on next graphs, where supply system currents are variable in time and the nominal torque is achieved at nominal speed.
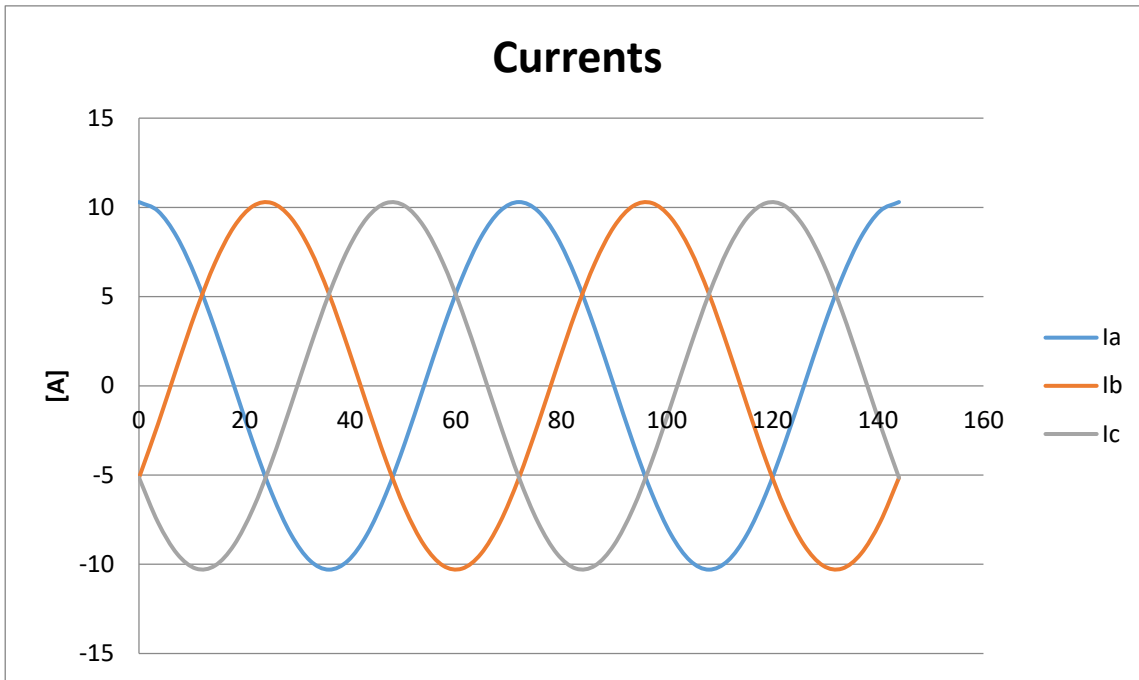
Figure 6.11– Currents
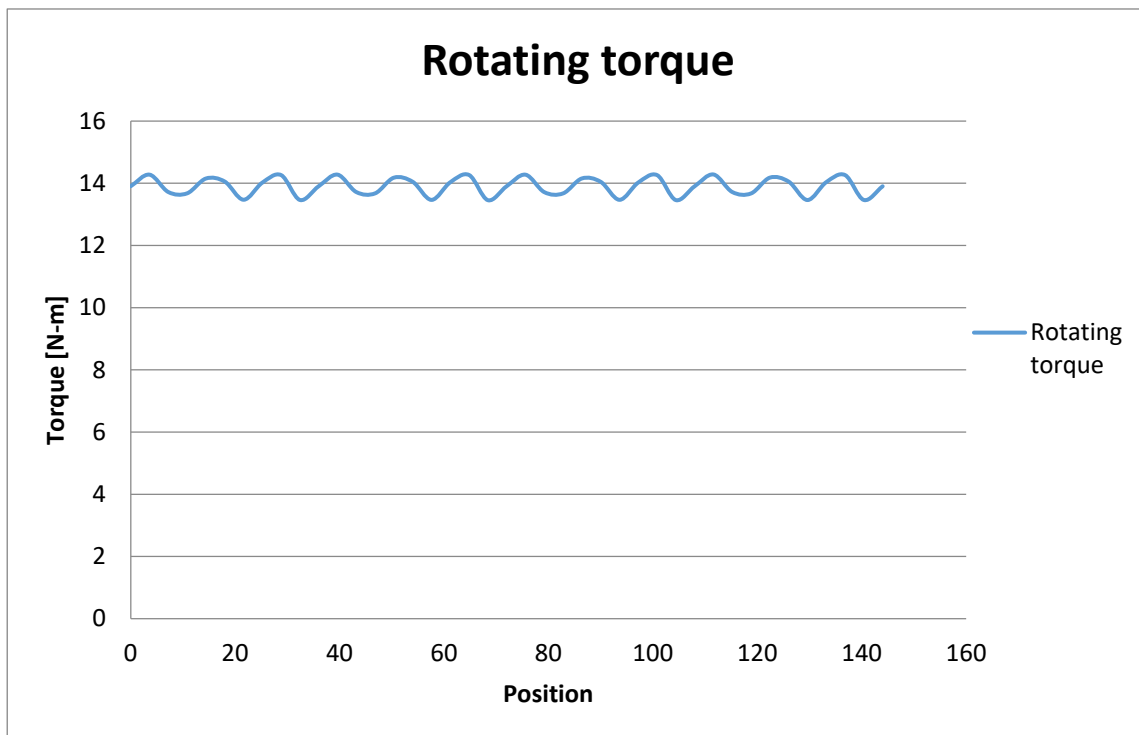
Figure 6.12– Rotating Torque. With nominal current variable in time, achieves the nominal torque

6.6. Inductances

In order to determine the inductances in the machine, the magnetic field energy located in the air gap, in the PM and the free space, and in the coils has to be calculated.

6.6.1. Simulation

The simulation performed has to be with the nominal current feeding the machine. The PM have to be canceled, by introducing to the coercivity field "hc" of the magnets a 0 value. This way only the inductance produce by the coils can be take into account.

The LUA script used is:

```lua
--Calculation of Ld and Lq with the Magnetic Field Energy

p=5
periode=360/p
step=periode/20

--File creation
handle=openfile("Results Magnetic Field Energy.txt", "a")
write(handle, "deg ", "Energy ", "\n")
closefile(handle)

for deg=0, 2*periode, step do

  mi_analyze();
  mi_loadsolution();

  handle=openfile("Results Magnetic Field Energy.txt","a")

  --select windings, PM+air and gap
  mo_groupselectblock(7)
  mo_groupselectblock(8)
  mo_groupselectblock(9)
  mo_groupselectblock(99)
  mo_groupselectblock(88)

  --Magnetic Field Energy
  E=mo_blockintegral(2)

  --Store in file
  write(handle,deg," ",E, "\n")
  closefile (handle)
  mo_close()

  --Motor rotation
  mi_seteditmode("group")
```

UNIVERSITAT POLITÈCNICA DE CATALUNYA
BARCELONA**TECH**
Escola d'Enginyeria de Barcelona Est

```
  mi_selectgroup(99)
  mi_selectgroup(70)
  mi_moverotate(0,0,step)
end
```

6.6.2.   Results

Once the magnetic field values are obtained, the Ld and Lq inductances can be calculated with the following expression of the definition of the magnetic field energy:

$$W = \frac{m}{2} \cdot L_m \cdot I^2_m$$

[6.3]

Knowing that the magnetic field energy is minimum by the d-axis and maximum by the q-axis, the expression that will determine the inductances are:

$$L_d := \frac{W_{min}}{\frac{m}{2} \cdot In^2}$$

[6.4]

$$L_q := \frac{W_{Max}}{\frac{m}{2} \cdot In^2}$$

[6.5]

Resulting in:

Ld= 0,012002

Lq= 0,019279

The magnetic field energy through the period of a pair of poles is shown on the next graph:

UNIVERSITAT POLITÈCNICA DE CATALUNYA
BARCELONATECH
Escola d'Enginyeria de Barcelona Est
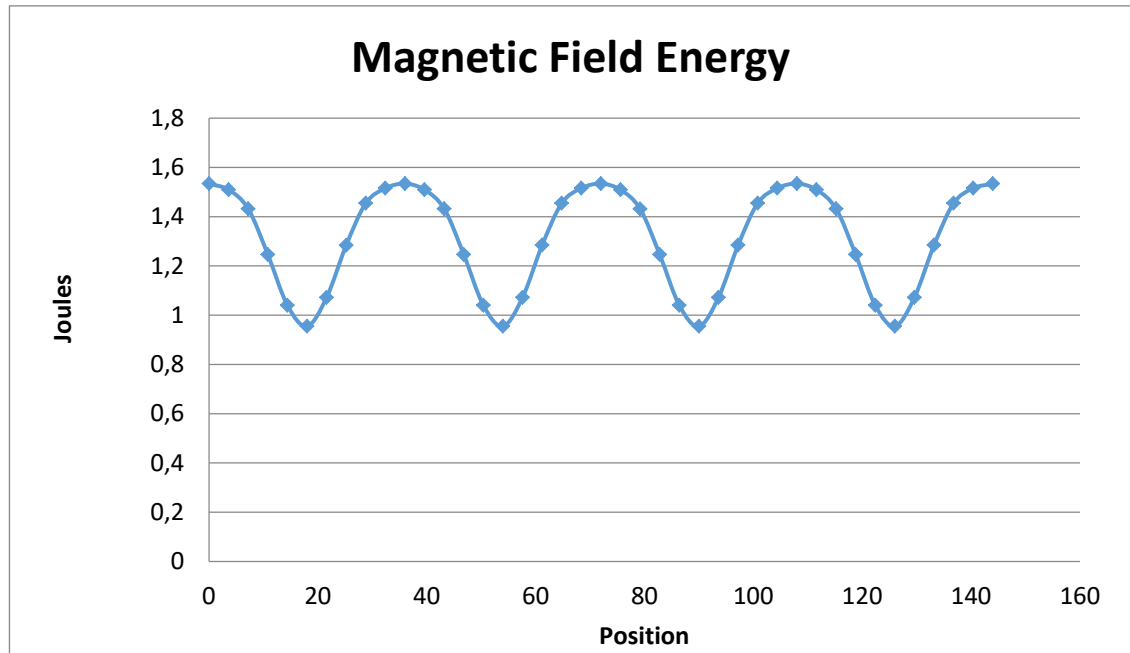
Figure 6.13– Magnetic field energy located in the airgap, the coils, and the PM and free spaces

6.7. Losses

The iron losses in the rotor and stator of the machine can be calculated through a simulation using the analytical expression from Bertotti.

$$P_{fe} = \frac{1}{\gamma}(K_h \cdot f \cdot B^2 + K_c \cdot f^2 \cdot B^2 + K_a \sqrt{f^3 \cdot B^3})$$

[6.5]

Where;

- γ = specific iron density
- f= frequency
- B=induction
- Kh, Kc, Ka are coefficient that have to be determine for each material.

In order to determine this coefficients, the specific characteristic "B - Losses[W/kg]" has to be take into account. In this case, the coefficients were calculated for the iron M470 50A. The methodology is to find the coefficients by reducing the error between the calculated losses from expression [6.5],

and the ones from the material characteristics. The Excel add-in tool "Solver" was used to calculate them.

Material	M470-50A					kc	0,542828
f	50		sumaerror	0,111851945		kh	203,7494
B	Pfe (W/kg)	PfeCalc (W/kg)		error^2		ka	8,351784
0	0	0		0		Densidad	7600
0,1	0,03	0,027476471		6,3682E-06		σ	330000
0,2	0,12	0,095511605		0,000599681		d	0,001
0,3	0,25	0,200553079		0,002444998			
0,4	0,42	0,341333246		0,006188458			
0,5	0,61	0,517119474		0,008626792			
0,6	0,82	0,727417442		0,00857153			
0,7	1,05	0,971864255		0,006105195			
0,8	1,3	1,250178741		0,002482158			
0,9	1,57	1,562134686		6,18632E-05			
1	1,87	1,90754495		0,001409623			
1,1	2,21	2,286251358		0,00581427			
1,2	2,59	2,698117914		0,011689483			
1,3	3,01	3,143026056		0,017695932			
1,4	3,53	3,620871215		0,008257578			
1,5	4,13	4,131560266		2,43443E-06			
1,6	4,78	4,675009577		0,011022989			
1,7	5,39	5,251143499		0,019281128			
1,8	5,82	5,859893169		0,001591465			

$$P_{fe} = \frac{1}{\gamma}(K_h \cdot f \cdot B^2 + K_c \cdot f^2 \cdot B^2 + K_a \sqrt{f^3 \cdot B^3})$$

$$K_c = \frac{\sigma \cdot \pi^2 \cdot d^2}{6}$$

Figure 6.14– Solver tool used to find the Bertotti`s coefficients

In the image above can be seen the characteristic losses from the material and the calculated ones. Modifying the coefficient values, the tool finds the parameters that minimize the error between the two curves. The Kc coefficient depends only from the material, where "d" refers to the considered width of the material and "σ" to the mechanical stress characteristic.

The Joule losses can be directly seen in the result window post-processor of FEMM.

6.7.1. Simulation

The iron losses results were obtained with the same simulation performed to determine the rotation torque, explained on point 6.5, but adding to the LUA script the following commands:

```
--Iron losses calculation
-- Static Method

freq=125
depth=0.09
--Bertotti Coefficients M470-50
Kc=0.542828
Kh=203.7494
Ka=8.351784


for deg=0, 2*periode, step do
```

UNIVERSITAT POLITÈCNICA DE CATALUNYA
BARCELONATECH
Escola d'Enginyeria de Barcelona Est

```
    Pfes=0
    Pfer=0
    Ia=Imax*cos(alfa*pi/180)
    Ib=Imax*cos(alfa*pi/180-2*pi/3)
    Ic=Imax*cos(alfa*pi/180+2*pi/3)
    mi_modifycircprop("A",1,Ia);
    mi_modifycircprop("B",1,Ib);
    mi_modifycircprop("C",1,Ic);

    mi_analyze(1)
    mi_loadsolution()

       --Stator Losses
    mo_smooth("off")
    numelm=mo_numelements()

    for k=1, numelm do
    --properties of each element
    --p1, p2, p3: magnetic potencial in each triangle vertex
    --x,y: triangle center coordinates
    --a: element area
    --g:element group

    p1,p2,p3,x,y,a,g=mo_getelement(k)
    if (g==2) then
       --element volume
       dv=depth*a*mm^2
       --center properties
       a,bx,by,sig,e,hx,hy=mo_getpointvalues(x,y)
       Bx=abs(bx)
       By=abs(by)
       Bmod=sqrt(Bx^2+By^2)

       --LOSSES
       Pfes=Pfes+(Kh*freq*Bmod^2+Kc*(freq*Bmod)^2+Ka*(freq*Bmod)^1.5)*dv
    end

--Rotor losses
   --properties of each element
   --p1, p2, p3: magnetic potencial in each triangle vertex
   --x,y: triangle center coordinates
   --a: element area
   --g:element group
   p1,p2,p3,x,y,a,g=mo_getelement(k)

   if (g==99) then
      --element volumen
      dv=depth*a*mm^2
      --center properties
      a,bx,by,sig,e,hx,hy=mo_getpointvalues(x,y)
      Bx=abs(bx)
      By=abs(by)
      Bmod=sqrt(Bx^2+By^2)
      --LOSSES
      Pfer=Pfer+(Kh*freq*Bmod^2+Kc*(freq*Bmod)^2+Ka*(freq*Bmod)^1.5)*dv
   end
end
   mi_seteditmode("group")
```

UNIVERSITAT POLITÈCNICA DE CATALUNYA
BARCELONATECH
Escola d'Enginyeria de Barcelona Est

```
mi_selectgroup(99)
mi_moverotate(0,0,step)
alfa=alfa+p*step

--store on file
handle=openfile("Resultados pérdidas.txt","a")
write(handle, deg,"  ", Pfes," ", Pfer, "\n")
closefile(handle)
mo_close()

end
```

6.7.2.   Results

The results obtained are shown on the next graph.
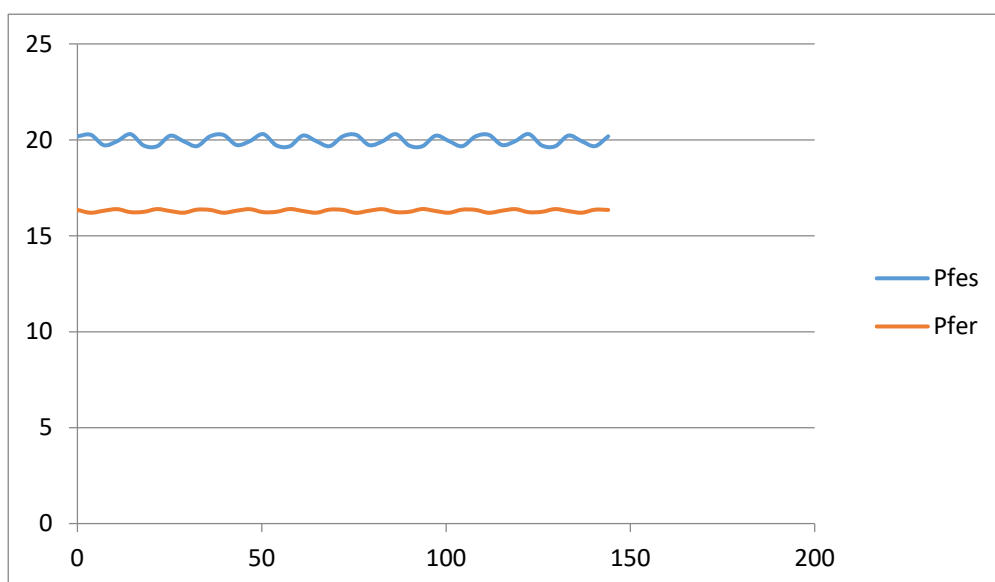
Figure 6.15– Iron losses

6.8.   Characteristics obtained

Once all the main parameters of the machine were obtained, the characteristics of the machine can be calculated.

UNIVERSITAT POLITÈCNICA DE CATALUNYA
BARCELONATECH
Escola d'Enginyeria de Barcelona Est

To understand the characteristic of these types of machine, the current model is used. The current has to be discomposed in de d-component and the q-component. These types of motors work on the second quadrant:
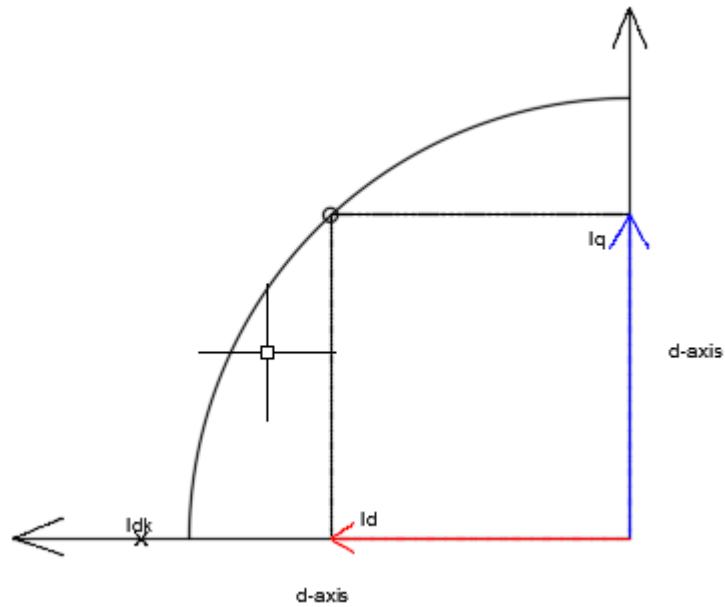
Figure 6.16– Discomposed currents

If the Idk current is bigger than the nominal current, the machine is considered theoretically as a finite speed machine. Being Idk: Ld/λ. And λ=E/2πf.

The expressions used to determine the characteristics depending on the speed are the followings:

$$M(\omega):=m\cdot p\cdot\left(\lambda\cdot I_q(\omega)+(L_d-L_q)\cdot I_d(\omega)\cdot I_q(\omega)\right)$$

[6.6]

$$U(\omega):=\omega\cdot\sqrt{\left(\lambda+L_d\cdot I_d(\omega)\right)^2+\left(L_q\cdot I_q(\omega)\right)^2}$$

[6.7]

$$P(\omega):=M\cdot\frac{\omega}{p}$$

[6.8]

There are two well differentiated working areas of the machine.
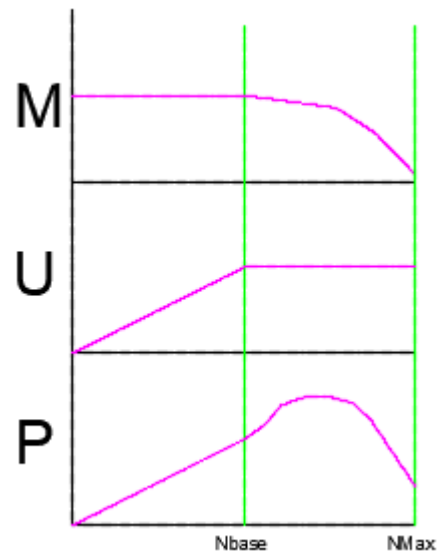
Figure 6.17– Working points of the machine

At the base speed "Nbase" the conditions are the nominal ones. It can be calculated with the expression:

$$\omega_{base} := \frac{U}{\sqrt{\left(\lambda + L_d \cdot I_{d0}\right)^2 + \left(L_q \cdot I_{q0}\right)^2}}$$

[6.9]

Until the base speed, the Id and Iq currents are constant and with value:

$$I_{d0} := \frac{-\lambda + \sqrt{\lambda^2 + 8\left(L_d - L_q\right)^2 \cdot I^2}}{4 \cdot \left(L_d - L_q\right)}$$

[6.10]

$$I_{q0} := \sqrt{I^2 - I_{d0}^2}$$

[6.11]

After the nominal speed, the currents begin to change its values. Id increase and Iq decrease, but In remain constant, so the torque start to decrease, but it still, the power generated by the machine increases. The current values for this situation are:

$$I_q := \frac{\sqrt{\left(\dfrac{U}{\omega}\right)^2 - \left(\Delta I_d \cdot L_d\right)^2}}{\delta \cdot L_d}$$

[6.12]

$$I_d := \sqrt{I^2 - I_q^2}$$

[6.13]

Where,

$$\delta := \frac{L_q}{L_d}$$

$$\Delta I_d := \frac{\delta \cdot \lambda + \sqrt{\left(\delta \cdot \lambda\right)^2 + 8 \cdot \left(1 - \delta\right)^2 \cdot \left(\dfrac{U}{\omega}\right)^2}}{4 \cdot \left(1 - \delta\right) \cdot \left(\dfrac{U}{\omega}\right)}$$

[6.14]

6.8.1.   Results

All this equations determine the characteristics of the machine. If the parameters are analyzed respect the speed of the machine, the followings graphs show the results obtained.
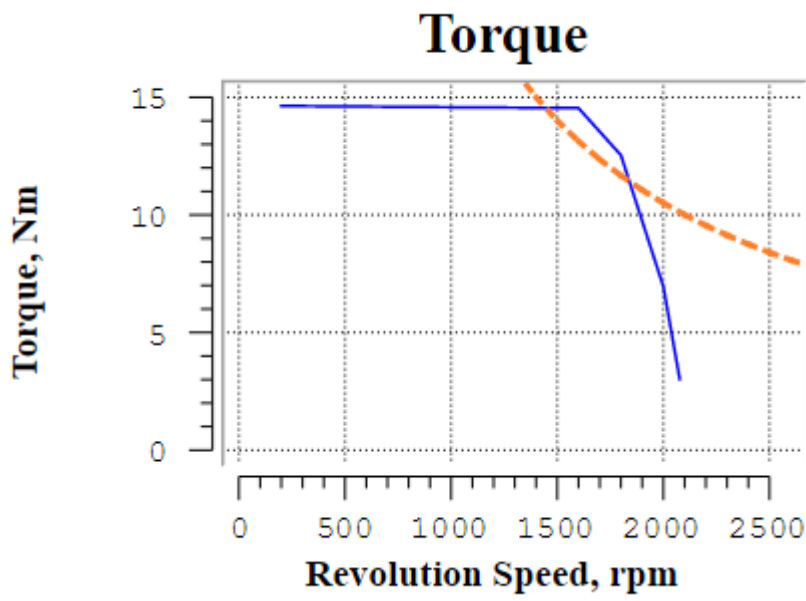
Torque

Figure 6.18– Torque
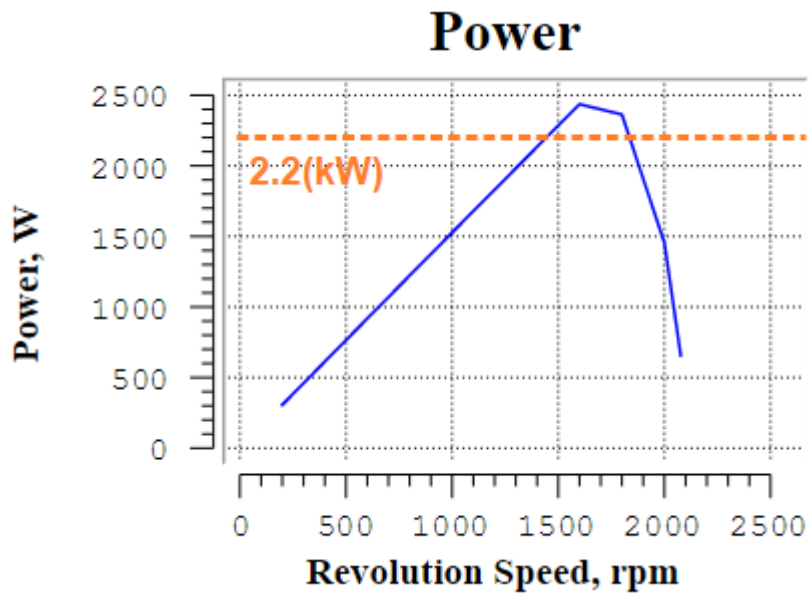
Power

Figure 6.19– Power
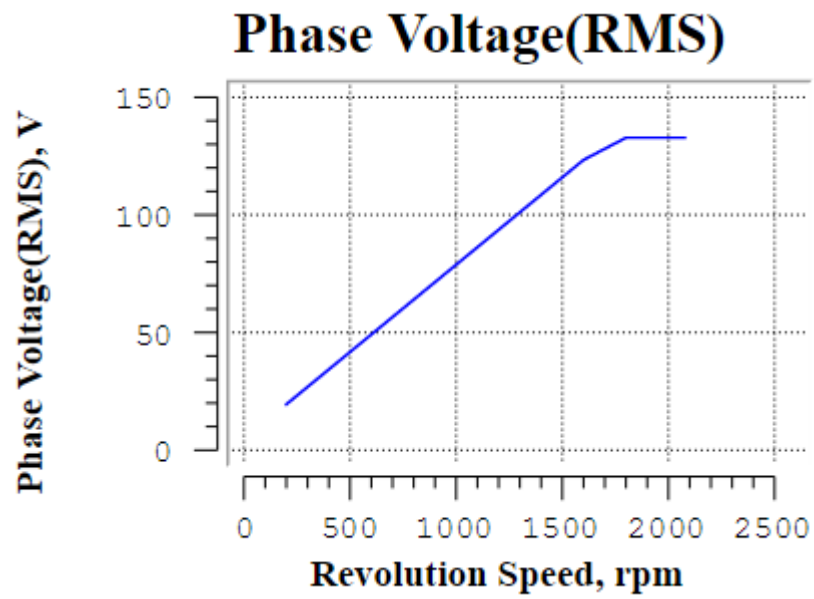
Figure 6.20– Voltage
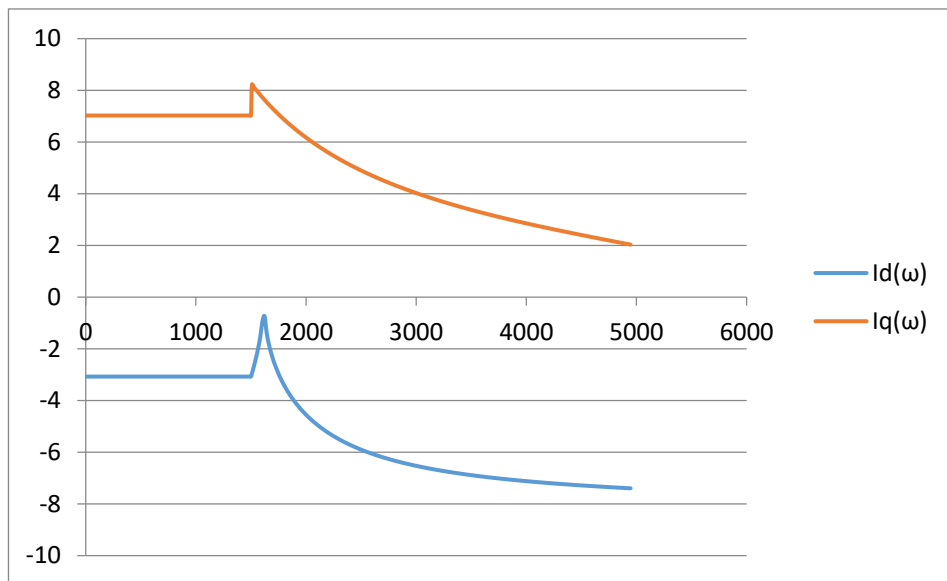
Figure 6.21– Id and Iq currents

6.9.   Thermal analysis: Heat flow problem

With FEMM it is possible to simulate not only electromagnetic problems, but also heat flow problems. Note: The casing of the motor is a generic casing draw, not a specific one, but to perform the simulation is believed as enough.

Once the motor and the chosen casing were draw in FEMM, it is necessary to define the materials. In this case the materials are defined by its losses and thermal characteristics. After obtaining the losses, and set them to unity per volume [W/m^3], this value can be introduced as "Volume Heat Generation". In the simulation is also taken into account the insulation film covering the coils, defined also as material with insulating characteristics.

One of the most important points to configure the model is to set the correct boundary conditions to all regions that are in touch with the fluid, in this case air. There ar going to be to defined convection conditions. One for the casing-atmosphere air convection, and other for the stator-rotor convection, setting the temperatures to the normalized values.

The model created is shown on next figure:
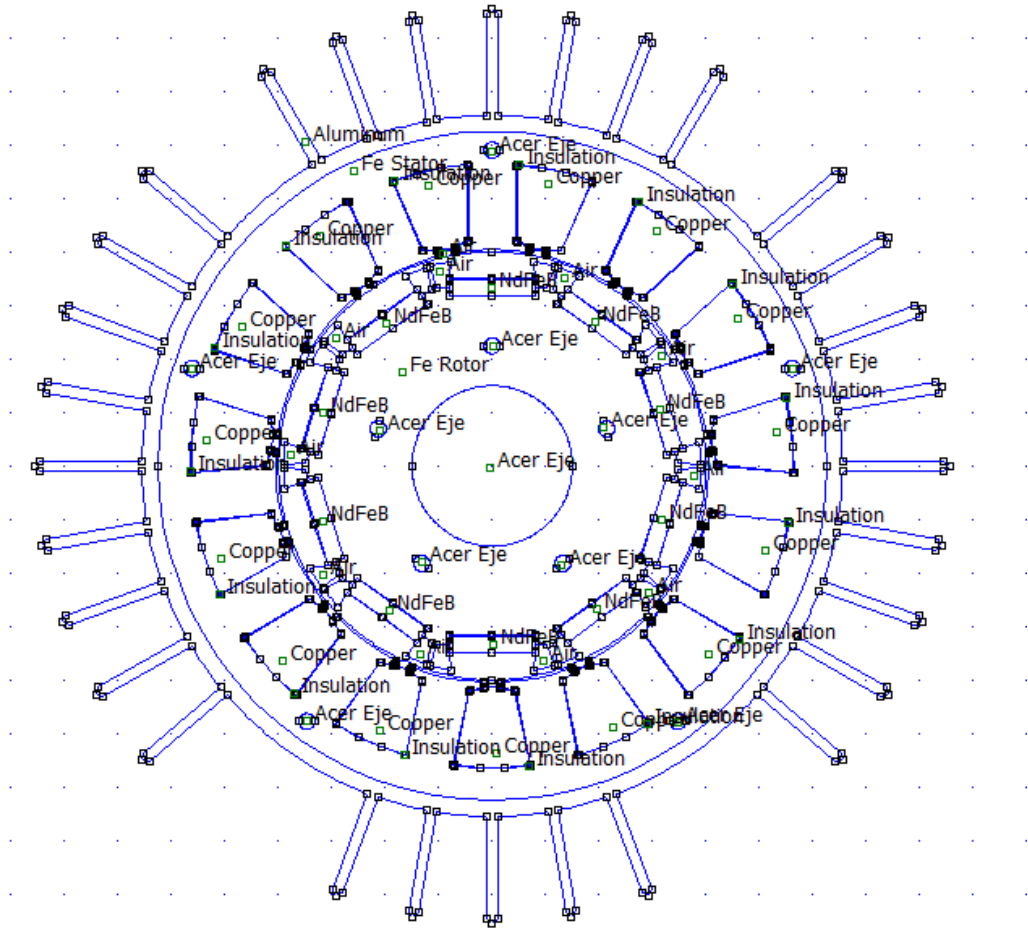
Figure 6.23– Model to perform the thermal analysis

6.9.1.   Results

After running the simulation with all parameters set, the obtained results are shown next, where it can be observed how the exterior temperatures are lower than 50°C, result of a good heat evacuation. The inner temperatures are lower than 150°C.
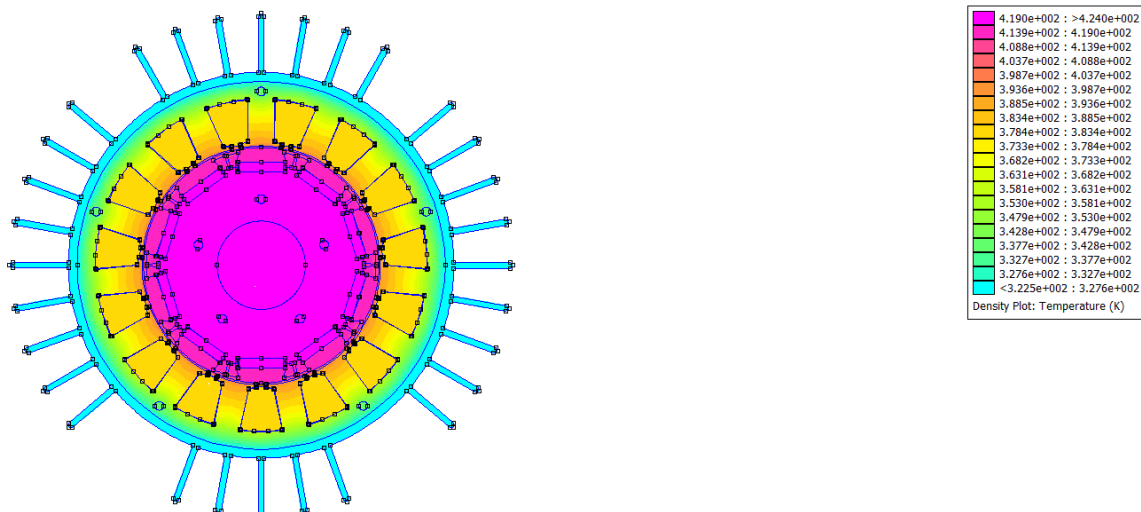
Figure 6.24– Results of the thermal analysis

6.10. FEMM Results

Some of the results obtained can be observed in the following table.

FEMM Analysis	
Torque [N.m]	14,1
Power [W]	2215
Phase Voltage[V]	117
Phase Current [A]	7,3
Copper Loss [W]	19,96
Iron Loss [W]	16,3
Ld [H]	1,20E-02
Lq [H]	0,01928
Number of turns per coil	37

UNIVERSITAT POLITÈCNICA DE CATALUNYA
BARCELONATECH
Escola d'Enginyeria de Barcelona Est

7. Environmental impact

As explained in the introduction chapter, the PMSM are very efficient machines and can deliver same torque as asynchronous machines in less volume and with fewer losses, characteristic that convert this types of machines in a very interesting option. These characteristics are mainly due to the use of this type of rare-earth permanent magnets.

The main problem of building a PMSM is the high and very variable cost of the rare-earth magnetic materials. In the last 6 months, the cost of these types of magnets has increased a 45%.

This is due to the fact, that almost the 100% of the extraction of these materials is performed in China. So, China controls the market. With the monopoly created, China can decide the costs fluctuations as desired, an even exert political pressures on big companies and governments. Such is the example of the Japanese company Toyota a few years ago, when China decided to decrease the extraction of rare-earths materials, increasing a lot the cost of them. Toyota had a diplomatic conflict with the Chinese government, and this decided to block the material exportation to Japan. To illustrate an idea, one single Toyota Prius engine has more than 11 kg of rare-earth materials. But not only cars, almost all the new technologies incorporate big amounts of these materials.

These rare-earth materials are so important in the growing technologies, and the dependency from China so strong, that the Japanese government even thought of building extraction platforms offshore, to obtain the materials at enormous depths, projects that will cost unimaginable amounts of money. And Toyota started to invest a lot of money in creating new technology engines with same characteristics, but less rare-earth material.

On the other hand, China government said that the measure adopted was in order to reserve material for the future, and because of environmental problems. The extraction of these materials involves the use of very pollutant chemicals, and it is performed on open sky mines, fact that allows very contaminant gases reach out to the atmosphere.

An alternative could be the use of Ferrite magnets. There is no global market issue with it and it is cheaper, but instead much more volume of material is needed to obtain the same characteristics. Anyway, as the demand increases, and such a market problem takes the scene, new technologies are being studied to avoid such a big volume of rare-earth materials.

UNIVERSITAT POLITÈCNICA DE CATALUNYA
BARCELONA**TECH**
Escola d'Enginyeria de Barcelona Est

8. Conclusions

After performing the simulations it can be said, that the results obtained are very similar to the ones analytical calculated, a very similar to the ones obtained with JMAG. This similarity is obviously due to the fact, that the analytical theories behind the different calculation methods are the same.

The analytical calculations of the machine are approximate, because they do not take into account many variables and possible micro malfunctioning's, or even the exact geometry of the armatures. But they really help to start a design process or to obtain the rated characteristics of a machine.

On the other hand, JMAG helps to accurate the analytical results, by introducing the parameters and obtaining almost real results. That is because JMAG takes in to account many other variables, that cannot be analytical calculated. Almost all result values were taken from JMAG to proceed with the design process.

Finally, FEMM, through the Finite Element Method, allows to introduce the accurate parameters obtained in JMAG and run the simulations, delivering the most real results, if all parameters and variables are well defined.

It is a fact, that a machine can be well design with the tools and methodology described in this work. It will not deliver 100% real results, as in other paid license software's, but if the calculations and simulations are carefully performed, a very acceptable design will be achieved.

9. Economic analysis and material executing budget

As explained on the point 7 of the present work, there is a considerable issue with the political and economic market of the rare-earth materials. The cost of the magnets is relatively low, because there is no much material used in small motors, but if its compare to the total cost of the machine, the magnets represent and important percentage . All the materials shown on the budget have the price of having them bought in China. The following table resumes how much it will be the design and construction of a prototype.

BUDGET				
2,2 kW Interior PMSM				
Item	**Quantity**	**Unitary Cost**	**Subtotal**	**Percentge**
Armatures	**kg**	**€/kg**		42,86%
Stator Iron [kg]	3,162	8	25,30 €	24,22%
Rotor Iron [kg]	2,433	8	19,46 €	18,64%
Magnets	**kg**	**€/kg**		**14,89%**
Neodimiun [kg]	0,3456	45	15,55 €	14,89%
Coils	**kg**	**€/kg**		**11,61%**
Copper [kg]	2,021	6	12,13 €	11,61%
Frame structure	**U.**	**€/U.**		**11,49%**
Casing	1	12	12,00 €	11,49%
Various	**U.**	**€/U.**		**19,15%**
Bearings, Insulation, Screws	1	20	20,00 €	19,15%
Working hours	**hs**	**€/hs**		
Engineering	20	12	240,00 €	
Assembler operator	12	8	96,00 €	
Total Material Budget			104,44 €	100,00%
TOTAL			440,44 €	

Table 9.1– Prototype costs

Prototype Total Costs = 440,44 €

UNIVERSITAT POLITÈCNICA DE CATALUNYA
BARCELONA**TECH**
Escola d'Enginyeria de Barcelona Est

But if we think of a motor in chain production, the engineering cost and the construction cost (working hours) decrease. The engineering cost can be divided between the units produced per year, and taking into account the amortization of the project through the years it will decrease even more. The resume of the costs of the motor in production and the final selling price is:

BUDGET 2,2 kW Interior PMSM				
Item	Quantity	Unitary Cost	Subtotal	Percentge
Armatures	**kg**	**€/kg**		**32,79%**
Stator Iron [kg]	3,162	8	25,30 €	24,22%
Rotor Iron [kg]	2,433	8	19,46 €	18,64%
Magnets	**kg**	**€/kg**		**11,39%**
Neodimiun [kg]	0,3456	45	15,55 €	11,39%
Coils	**kg**	**€/kg**		**8,88%**
Copper [kg]	2,021	6	12,13 €	8,88%
Frame structure	**U.**	**€/U.**		**11,49%**
Casing	1	12	12,00 €	11,49%
Various	**U.**	**€/U.**		**19,15%**
Bearings, Insulation, Screws	1	20	20,00 €	19,15%
Working hours	**hs**	**€/hs**		
Engineering	20	12	0,05 €	
Assembler operator	4	8	32,00 €	
Units/year (amortization)	5000			
Benefit %	20			
Total Material Budget			136,49 €	83,71%
PRICE			170,61 €	

Table 9.2– Selling price

UNIVERSITAT POLITÈCNICA DE CATALUNYA
BARCELONATECH
Escola d'Enginyeria de Barcelona Est

10. Bibliography

- Fraile Mora, J., 2015. MÁQUINAS ELÉCTRICAS. 7ma Edición. Ibergarceta Publicaciones, S.L. ISBN: 978-84-1622-813-3

- Bueno, B., 2015. REGLAMENTO ELECTROTÉCNICO PARA BAJA TENSIÓN. 2da Edición. Marcombo. ISBN: 978-84-267-2254-6

- Bargalló Perpinà, R., Sust, J., Morón, J. Pujolras, J.C. Paper: Analysis of PMSM using FE: A didactical approach for EMF determination and cooging torque reduction.

- Bargalló Perpinà, R. 2017. Apuntes de clase y material de estudio. Asignaturas: Máquinas eléctricas 1, Máquinas Eléctricas 2, y Diseño de máquinas eléctricas.

- Yeste, G, Fillet, S. 2016. Apuntes y material de estudio. Asignatura: Electric Drives

- Bibhu P. Panigrahi. Patra, K.C. 1999. Design of a permanent magnet synchronous machine motor. Taylor and Francis, Inc.

- Qinghua, L. 2005. Thesis: Analysis, design and control of permanent magnet synchronous motors for wide speed operation.

- Barta, J. Paper: Computer aided rotor design and simulation of synchronous reluctance machine.

- Meeker, D. 2015. Finite Element Method Magnetics – Users Manual

11. Annex A

11.1. Analytical calculations

InitialDimensions

$P_n := 2200 \qquad p := 5 \qquad \eta := 0.914 \qquad H_c := 979000 \qquad \mu_0 := 4 \cdot \dfrac{\pi}{10^7} = 1.257 \cdot 10^{-6}$

$N_n := 1500 \qquad m := 3 \qquad\qquad\qquad B_r := 1.28$

$f_s := p \cdot \dfrac{N_n}{60} = 125 \qquad\qquad\qquad\qquad\qquad \mu_r := \dfrac{B_r}{\mu_0 \cdot H_c} = 1.04$

$M_n := \dfrac{P_n}{\left(\dfrac{2 \cdot \pi}{60}\right) \cdot N_n} = 14.006$

Typical Prototype Waveforms

$K_e := \sqrt{2}$

$K_i := \sqrt{2}$

$K_p := 0.5$ Long/diam $K_I := \dfrac{p^{\left(\frac{-2}{3}\right)} \cdot \pi}{2} = 0.537$

Current layer for the design $A_s := 18000$

Magnet remain Ind $B_r = 1.28 \qquad B_{av} := 0.75 \cdot B_r = 0.96$

$$D_e := \sqrt[3]{2 \cdot p \cdot \frac{P_n}{m \cdot A_s \cdot K_e \cdot K_i \cdot K_p \cdot K_l \cdot \eta \cdot B_{av} \cdot \pi \cdot f_s}} = 0.13$$

Outer diameter fix:

$$D_e := 0.125$$

$$L := \frac{2 \cdot p \cdot P_n}{m \cdot A_s \cdot K_e \cdot K_i \cdot K_p \cdot D_e^2 \cdot \eta \cdot B_{av} \cdot \pi \cdot f_s} = 0.076$$

Longitud taken beacuse of heating
calculations: 0,9

Initial Characteristics

$P_n := 2200$	$p := 5$	$\eta := 0.914$	$U := 230$	$d_i := 0.03$	$D_i := 0.081$
$N_n := 1500$	$m := 3$	$cos\varphi := 0.8$	$Q := 15$	$d_e := 0.08$	$D_e := 0.125$
	$\Delta := 6$				$L := 0.09$
$b_m := 0.016$					$g := 0.5$
$h_m := 0.0032$					

$$M_n := \frac{P_n}{\left(\frac{2 \cdot \pi}{60}\right) \cdot N_n} = 14.006 \qquad\qquad TRV := \frac{M_n}{\frac{\pi}{4} \cdot D_i^2 \cdot L} = 3.02 \cdot 10^4$$

$$fs := p \cdot \frac{N_n}{60} = 125 \qquad\qquad \omega := \frac{2 \cdot \pi}{60} \cdot N_n = 157.08$$

$$\omega := 2 \cdot \pi \cdot fs = 785.398$$

$$Udc := U \cdot 1.35 = 310.5$$

$$U_{Lmax} := \frac{4}{\pi} \cdot Udc = 395.341$$

$$Un_f := \frac{U_{Lmax}}{\sqrt{3}} = 228.25 \qquad\qquad U_n := \frac{Un_f}{\sqrt{2}} = 161.397$$

Altern

$$U_n := \frac{U}{\sqrt{3}} = 132.791 \qquad\qquad U_{lmax} := 230 \cdot \sqrt{2} = 325.269 \quad \text{Line Voltage Peak (JMAG)}$$

$$In := \frac{P_n}{m \cdot U_n \cdot \eta \cdot cos\varphi} = 7.553 \qquad\qquad q := \frac{Q}{2 \cdot p \cdot m} = 0.5$$

$$I_{max} := In \cdot \sqrt{2} = 10.681$$

UNIVERSITAT POLITÈCNICA DE CATALUNYA
BARCELONATECH
Escola d'Enginyeria de Barcelona Est

Air gap induction

$$\tau_p := \frac{\pi \cdot d_e}{2 \cdot p} = 0.025$$

Opening between magnets (on the airgap arc)

$$b_g := \frac{\pi \cdot d_e}{40} = 0.006$$

Carter Factor

$$g := 0.0005$$

$$k_c := \frac{\tau_p}{\tau_p - \frac{b_g^2}{5 \cdot g + b_g}} = 1.218$$

$H_c := 979000$

$\mu_0 := 4 \cdot \frac{\pi}{10^7} = 1.257 \cdot 10^{-6}$

Slot distance to diameter

$x := 0.001$

$B_r := 1.28$

$B_{max} := 1$

$$\mu_r := \frac{B_r}{\mu_0 \cdot H_c} = 1.04$$

Eq. Airgap CARTER

$$g_c := g \cdot k_c = 6.089 \cdot 10^{-4}$$

Pole covering factor

$$\Psi := \frac{b_m}{\tau_p} = 0.637$$

In degrees:

$$\Psi := \frac{25}{\frac{360}{2 \cdot p}} = 0.694$$

$$B_e := \frac{B_r - B_{max} \cdot \frac{2 \cdot x}{b_m}}{g_c \cdot \frac{\mu_r}{h_m} + \frac{\Psi \cdot \pi \cdot d_e}{2 \cdot p \cdot b_m}} = 0.896$$

Flux

$$\Phi := \frac{2}{\pi} \cdot B_{max} \cdot \tau_p \cdot L = 0.001$$

Winding factor

$L = 0.09$
$\tau_p = 0.025$
$fs = 125$

$\xi_b := 0.866$ Software koil value

$E := 120$

$$N_f := \frac{E}{\frac{2 \pi}{\sqrt{2}} \cdot \xi_b \cdot \Phi \cdot fs} = 173.271$$

$N_f := 175$

$Z_t := 2 \cdot m \cdot N_f = 1.05 \cdot 10^3$

$$E := \frac{2 \pi}{\sqrt{2}} \cdot N_f \cdot \xi_b \cdot \Phi \cdot fs = 121.197$$

$$\lambda := \frac{E}{\omega} = 0.154$$

$$Z_r := \frac{Z_t}{Q} = 70$$

$$E := \frac{2 \pi}{\sqrt{2}} \cdot N_f \cdot \xi_b \cdot B_e \cdot d_e \cdot L \cdot \frac{fs}{p} = 108.615$$

$$N_b := \frac{N_f}{5} = 35$$

$$As := \frac{Z_t \cdot In}{\pi \cdot D_e} = 2.019 \cdot 10^4$$

Conductors Section $\qquad aa := 2 \qquad \Delta := 7.6 \qquad$ JMAG Value

$$S_c := \frac{In}{\Delta} = 0.994$$

$$d_c := \sqrt{\frac{4 \cdot S_c}{\pi \cdot aa}} = 0.795$$

Diam Election $\qquad d_c := 0.8$

Two wires fit: OK $\qquad\qquad Apertura := 0.003 \quad 2 \cdot d_c = 1.6 \quad$ <Apertura OK

$$S_{oc} := aa \cdot Z_r \cdot \pi \cdot \frac{d_c^2}{4} = 70.372$$

$$S_r := 171.4 \qquad$$ Foc needs to be 0.4. Values from JMAG (75% fill) OK

$$F_{oc} := \frac{S_{oc}}{S_r} = 0.411$$

$$S_c := \frac{aa \cdot \pi \cdot d_c^2}{4} = 1.005 \quad \Delta_{real} := \frac{In}{S_c} = 7.513$$

INDUCTANCES (Carter Eq. Airgap)

$$L_m := \frac{\mu_0}{\pi} \cdot m \cdot \frac{D_e \cdot L}{g_c} \cdot \left(\frac{N_f \cdot \xi_b}{p} \right)^2 = 0.02$$

$$k_q := \frac{(\Psi \cdot \pi - \sin(\Psi \cdot \pi))}{\pi} = 0.434$$

$$k_d := \left(\frac{\left(\sin\left(\frac{\Psi \cdot \pi}{2} \right) \right)^2}{\frac{\Psi \cdot \pi}{2} + p \cdot g_c \cdot \mu_r \cdot \frac{b_m}{h_m \cdot D_i}} \right) \cdot \frac{4}{\pi} - k_q = 0.345$$

$$L_m = 0.02$$

$$L_{mq} := L_m \cdot k_q = 0.009$$

$$L_{md} := L_m \cdot k_d = 0.007$$

UNIVERSITAT POLITÈCNICA DE CATALUNYA
BARCELONATECH
Escola d'Enginyeria de Barcelona Est

Stray Inductances

Slot

$$l_r = \mu_0 \cdot n^2 \cdot L \cdot \left(\frac{2 \cdot h_1}{3 \cdot (b_1 + b_3)} + \frac{(h_2 - h_1)}{b_3} + \frac{h_3 - h_2}{b_3 - b_4} \cdot \ln\left(\frac{b_2}{b_4}\right) + \frac{(h_4 - h_3)}{b_4} \right)$$
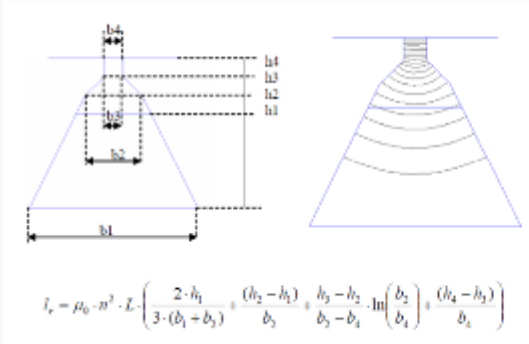
$$
\begin{array}{llll}
N := 35 & h_1 := 0.01176 & h_3 := 0.01506 & b_1 := 0.01442 & b_4 := 0.003 \\
L := 0.095 & h_2 := 0.01433 & h_4 := 0.01594 & b_2 := 0.00871 &
\end{array}
$$

$$L_r := \mu_0 \cdot N^2 \cdot L \left(\frac{2 \cdot h_1}{3 \cdot (b_1 + b_2)} + \frac{(h_2 - h_1)}{b_2} + \frac{(h_3 - h_2)}{b_2 - b_4} \cdot \ln\left(\frac{b_2}{b_4}\right) + \frac{(h_4 - h_3)}{b_4} \right) = 1.555 \cdot 10^{-4}$$

$$L_t := L_m + L_r = 0.021$$

$$L_{mq} := L_t \cdot k_q = 0.009$$

$$L_{md} := L_t \cdot k_d = 0.007$$

Losses and thermal analysis

$I := 7.238$ $N_f := 175$ $d_{caisla} := 0.884$ $l_{cond} := 0.09$ $D_e := 0.125$ $p := 5$

$aa := 2$

$$S_c := \frac{aa \cdot \pi \cdot d_{caisla}^2}{4} = 1.228 \qquad\qquad\qquad \tau_p := \frac{\pi \cdot D_e}{2 \cdot p} = 0.039$$

Coil av longitude
$$l_{esp} := 2 \cdot l_{cond} + 2.3 \cdot \tau_p = 0.27$$

Copper resistivity (at 100ºC)

$$\rho_{Cu20} := \frac{1}{58} = 0.017 \qquad\qquad a := 0.00393 \qquad T` := 100$$

$$\rho_{Cu100} := \rho_{Cu20} \cdot (1 + a \cdot (T` - 20)) = 0.023 \qquad\qquad \sigma_{Cu100} := \frac{1}{\rho_{Cu100}} = 44.127$$

$$R := N_f \cdot \rho_{Cu100} \cdot \frac{l_{esp}}{S_c} = 0.873 \qquad\qquad R := \frac{N_f \cdot l_{esp}}{\sigma_{Cu100} \cdot S_c} = 0.873$$

$$P_j := 3 \cdot R \cdot I^2 = 137.262$$

$$P_{fe} := \frac{1}{3} \cdot P_j = 45.754$$

$$Perd := P_j + P_{fe} = 183.016$$

Volumes (FEMM)

$V_{bob} := 0.000231$ $V_{fe} := 0.0007144$ $FEMMValues$

$$P_j := \frac{P_j}{V_{bob}} = 5.942 \cdot 10^5 \qquad P_{fe} := \frac{P_{fe}}{V_{fe}} = 6.405 \cdot 10^4$$

+

UNIVERSITAT POLITÈCNICA DE CATALUNYA
BARCELONATECH
Escola d'Enginyeria de Barcelona Est

Heating

$$D_e = 0.125 \qquad Esp_{carcasa} := 0.003 \qquad h_{cabezabob} := 4.15 \cdot 0.674 = 2.797 \qquad l_{tapa} := 0.02$$

$$D_{ext} := D_e + 2 \cdot Esp_{carcasa} = 0.131$$

Graphic calculation in Autocad. Aproximation through: $h_{cabezabob} := 0.02$

$$L_{carc} := l_{cond} + 2 \cdot h_{cabezabob} + l_{tapa} = 0.15$$

Vent Surface

$$S_v := D_{ext} \cdot L_{carc} \cdot \pi = 0.062 \qquad m2 \qquad 0.137 \cdot 10^3 = 137$$

Natural Convection $\qquad \Theta_{max} := 100$

$$K_v := 1.32 \cdot \sqrt[4]{\frac{1000 \cdot \Theta_{max}}{D_{ext} \cdot 10^3}} = 6.938 \qquad \frac{W}{C \cdot m2}$$

$Perd = 183.016$
$Losses := 150$

$$\Theta := \frac{Losses}{K_v \cdot S_v} = 350.205$$

With fins

$$N_{alet} := 28 \qquad h_{alet} := 0.02$$

$$+$$

$$S_{aletas} := N_{alet} \cdot 2 \cdot h_{alet} \cdot L_{carc} = 0.168$$

$$S_v := S_v + S_{aletas} = 0.23$$

$$K_v := 1.32 \cdot \sqrt[4]{\frac{1000 \cdot \Theta_{max}}{D_{ext} \cdot 10^3}} = 6.938 \qquad \frac{W}{C \cdot m2}$$

$$\Theta := \frac{Perd}{K_v \cdot S_v} = 114.818$$

Forced convection, with fan
$v := 5.5$ Considered at 1500rpm airspeed 5,5m/s

$$S_v := D_{ext} \cdot L_{carc} \cdot \pi = 0.062$$

$$K_v := 3.89 \cdot \sqrt{\frac{1000 \cdot v}{D_{ext} \cdot 10^3}} = 25.205 \qquad \frac{W}{C \cdot m2}$$

$$\Theta := \frac{Perd}{K_v \cdot S_v} = 117.62$$

Forced convection + fins
$N_{alet} := 38 \qquad\qquad h_{alet} := 0.02$

$$S_{aletas} := N_{alet} \cdot 2 \cdot h_{alet} \cdot L_{carc} = 0.228$$

$$S_v := S_v + S_{aletas} = 0.29$$

$$K_v := 3.89 \cdot \sqrt{\frac{1000 \cdot v}{D_{ext} \cdot 10^3}} = 25.205 \qquad \frac{W}{C \cdot m2}$$

$$\Theta_{max} := \frac{Perd}{K_v \cdot S_v} = 25.061$$

Final Characteristics, calculated in Excel with the followings expressions:

$P_n := 2200 \qquad\qquad p := 5 \qquad V := 230 \qquad E_M := 120 \qquad\qquad L_d := 0.009633$
$N_n := 1500 \qquad\qquad m := 3 \qquad I := 7.674 \qquad\qquad\qquad\qquad\qquad L_q := 0.01796$
$\qquad\qquad\qquad\qquad\quad \Delta := 6 \qquad\qquad\qquad U := \dfrac{V}{\sqrt{3}} = 132.791 \qquad$ Jmag

$$f := p \cdot \frac{N_n}{60} = 125 \qquad\qquad \Omega := \frac{2 \cdot \pi}{60} \cdot N_n = 157.08 \qquad\qquad \text{Initiate values. No importance}$$

$$\omega := 2 \cdot \pi \cdot f = 785.398 \qquad\qquad I_d := 1$$

$$\lambda := \frac{E_M}{\omega} = 0.153 \qquad\qquad \lambda := \frac{\lambda}{\sqrt{2}} = 0.108 \qquad\qquad \begin{aligned} I_q &:= 1 \\ M &:= 1 \end{aligned}$$

$$M(\omega) := m \cdot p \cdot \left(\lambda \cdot I_q(\omega) + (L_d - L_q) \cdot I_d(\omega) \cdot I_q(\omega) \right) \qquad I_q(\omega) := \sqrt{I^2 - I_d(\omega)^2}$$
$$\text{OK Salient Poles}$$

$$U(\omega) := \omega \cdot \sqrt{\left(\lambda + L_d \cdot I_d(\omega) \right)^2 + \left(L_q \cdot I_q(\omega) \right)^2} \qquad\qquad P(\omega) := M \cdot \frac{\omega}{p}$$

UNIVERSITAT POLITÈCNICA DE CATALUNYA
BARCELONATECH
Escola d'Enginyeria de Barcelona Est

92

$$I_{d0} := \frac{-\lambda + \sqrt{\lambda^2 + 8\,(L_d - L_q)^2 \cdot I^2}}{4 \cdot (L_d - L_q)} = -3.078$$

$$I_{q0} := \sqrt{I^2 - I_{d0}^2} = 7.03 \qquad U := \frac{V}{\sqrt{3}} = 132.791$$

$$\omega_{base} := \frac{U}{\sqrt{(\lambda + L_d \cdot I_{d0})^2 + (L_q \cdot I_{q0})^2}} = 893.581$$

$$f_{base} := \frac{\omega_{base}}{2 \cdot \pi} = 142.218 \qquad N_{base} := 60 \cdot \frac{f_{base}}{p} = 1.707 \cdot 10^3$$

$$\delta := \frac{L_q}{L_d}$$

$$\Delta I_d := \frac{\delta \cdot \lambda + \sqrt{(\delta \cdot \lambda)^2 + 8 \cdot (1 - \delta)^2 \cdot \left(\frac{U}{\omega}\right)^2}}{4 \cdot (1 - \delta) \cdot \left(\frac{U}{\omega}\right)}$$

$$I_q := \frac{\sqrt{\left(\frac{U}{\omega}\right)^2 - (\Delta I_d \cdot L_d)^2}}{\delta \cdot L_d}$$

$$I_d := \sqrt{I^2 - I_q^2}$$

UNIVERSITAT POLITÈCNICA DE CATALUNYA
BARCELONATECH
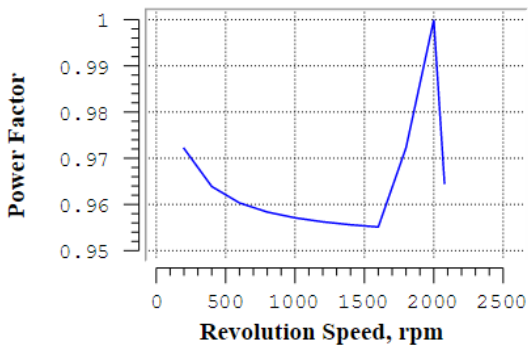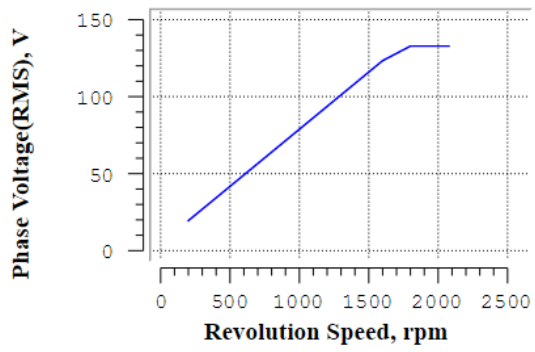Escola d'Enginyeria de Barcelona Est

12. Annex B
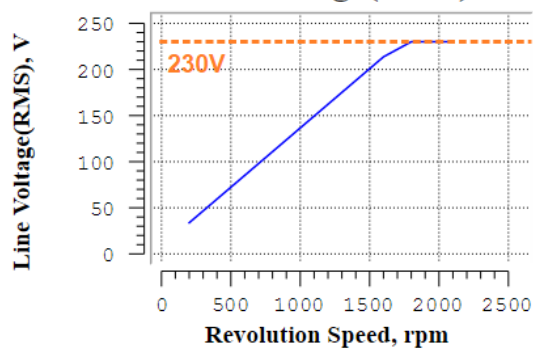
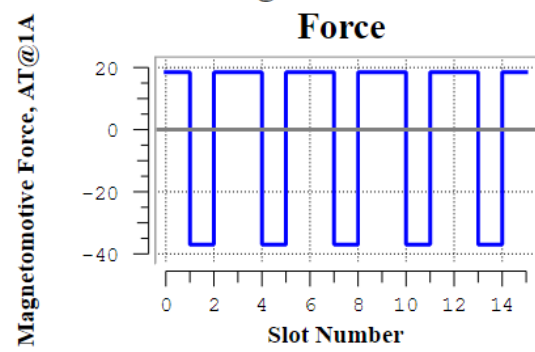## 12.1. JMAG Characteristics plots and results
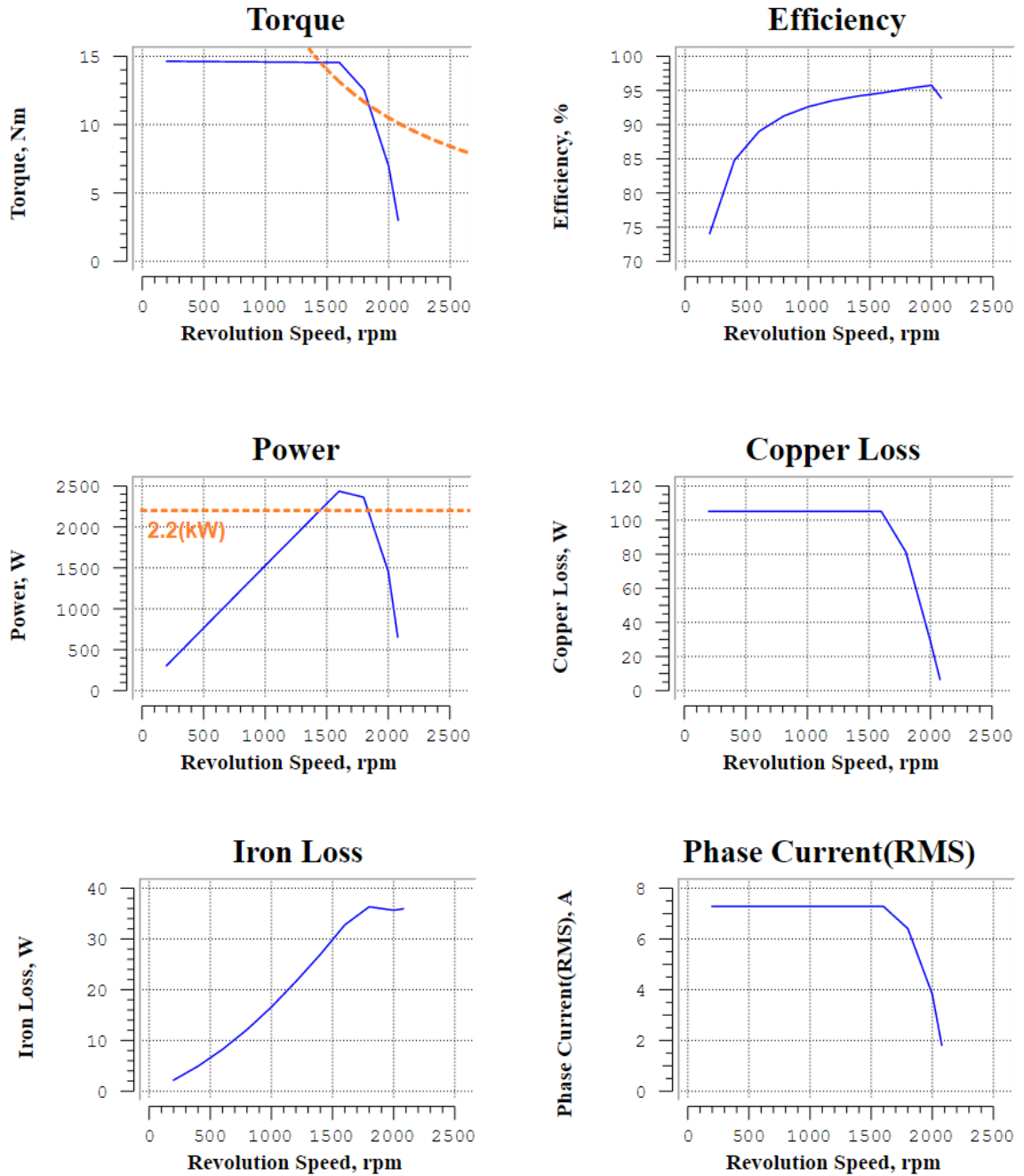
Power Factor

Phase Voltage(RMS)

Line Voltage(RMS)

Magnetomotive Force

Torque

Torque

UNIVERSITAT POLITÈCNICA DE CATALUNYA
BARCELONATECH
Escola d'Enginyeria de Barcelona Est
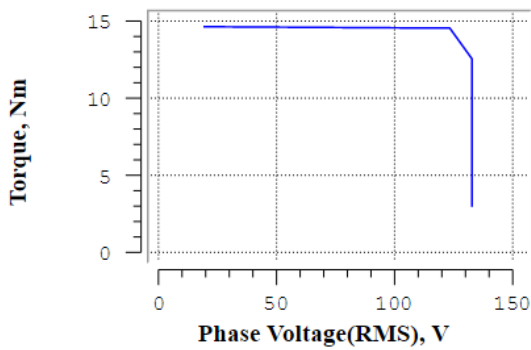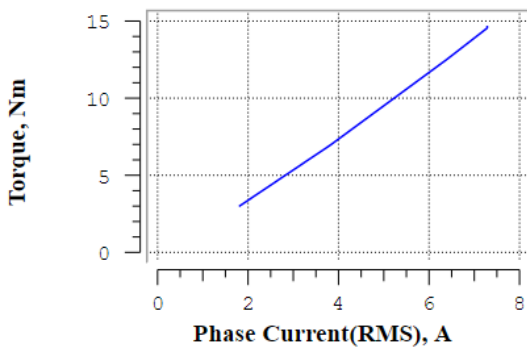
Machine Constant		
Revolution Speed	N, rpm	1500
Inductance	Ld, H	9.633e-03
	Lq, H	0.01796
	Self Inductance, H	9.196e-03
	Mutual Inductance, H	-4.598e-03
Torque Constant	Kt, Nm/A	1.488
Voltage Constant	Ke, V s/rad	1.718
Magnetic Circuit	Average Teeth Flux Density, T	0.9995
	Average Back Yoke Flux Density, T	0.7588
	Average Gap Flux Density, T	0.4957
Electric Part	Phase Current(RMS), A	7.283
	Wire Current Density, A/m^2	7.245e+06
Power	Torque, Nm	14.55
	Efficiency, %	94.41
	Power, W	2285
	Power Factor	0.9554
Loss	Copper Loss, W	105.1
	Iron Loss, W	29.85
Electric Circuit	Phase Voltage(RMS), V	115.9
	Line Voltage(RMS), V	200.8

| Winding	
Connection Type	Star Connection
Series Number	5
Parallel Number	1
Number of Turns	37
Setting Type	Round Wire Dimension
Wire Diameter, mm	0.8
Film Thickness, mm	0.1
Number of Strands	2
Insulation Thickness, mm	0.13
Slot-Fill Factor, %	74.08
Max Slot-Fill Factor, %	75
Correction Factor	1
Slot Area, mm^2	167.4
Conductor Area, mm^2	18.6
Phase Resistance, ohm	0.6606
Winding	Concentrated Winding
Coil Current Density(@1A), A/mm^2	0.9947

Drive	
Mode	Voltage(Sin)
Line Voltage(peak), V	325.3
Current Phase, deg	30
Maximum Line Current(peak), A	10.3
X-Axis	Revolution Speed, rpm

UNIVERSITAT POLITÈCNICA DE CATALUNYA
BARCELONATECH
Escola d'Enginyeria de Barcelona Est

Dimension		
All	Outer Diameter, mm	*125*
	Gap Length, mm	*0.5*
	Stack Height, mm	*90*
stator : **so_011**	Number of Slots	*15*
	Stator Outside Diameter, mm	*125*
	Stator Bore Diameter, mm	*81*
	Angle of Slot, deg	*24*
	Depth of Stator Slot, mm	*16*
	Width of Stator Slot-bottom, mm	*14.5*
	Width of Stator Slot-opening, mm	*3*
	Height of Stator Tooth-tang, mm	*1*
	Angle of Stator Tooth-tang, deg	*22*
	Fillet Radius at Stator Slot-bottom, mm	*0.25*
	Fillet Radius at Stator Slot-top, mm	*0.25*

Mass Property		
Total	Total Weight, kg	7.962
	Total Volume, mm^3	9.983e+05
Stator	Stator Core - Mass, kg	3.162
	Stator Core - Volume, mm^3	4.107e+05
	Coil - Mass, kg	2.021
	Coil - Volume, mm^3	2.255e+05
	Part Weight(so_011)	5.183
Rotor	Rotor Magnet - Mass, kg	0.3456
	Rotor Magnet - Volume, mm^3	4.608e+04
	Rotor Core - Mass, kg	2.433
	Rotor Core - Volume, mm^3	3.16e+05
	Part Weight(rip_000)	2.779
Inertia	Rotor Magnet, kg m^2	3.898e-04
	Rotor Core, kg m^2	2.063e-03
	Total, kg m^2	2.453e-03

ipm_rotor : **rip_000**	Number of Magnet Poles	*10*
	Outside Diameter, mm	*80*
	Shaft Diameter, mm	*30*
	Position of Magnet, mm	*31.65*
	Magnet Thickness, mm	*3.2*
	Magnet Width, mm	*16*
	Clearance between Slits, mm	*1*
	Slit Width, mm	*2.6*
	Slit Depth, mm	*1*

UNIVERSITAT POLITÈCNICA DE CATALUNYA
BARCELONA**TECH**
Escola d'Enginyeria de Barcelona Est

Materials		
Stator Core	Category	JSOL - Steel_Sheets
	Type	*50A470*
	Density, kg/m^3	7700
Coil	Category	Copper
	Density, kg/m^3	8960
	Drive Temperature, degC	*20*
	Base Temperature, degC	20
	Temperature Correction Factor, ppm/degC	3810
Rotor Magnet	Category	JSOL - NdFeB_Magnet
	Type	*NdFeB_Br=1.2(T)*
	Drive Temperature, degC	*20*
	Base Temperature, degC	*20*
	Temperature Correction Factor, %/degC	*0*
	Magnetization Pattern	Parallel
	Density, kg/m^3	7500
Rotor Core	Category	JSOL - Steel_Sheets
	Type	*50A470*
	Density, kg/m^3	7700

UNIVERSITAT POLITÈCNICA DE CATALUNYA
BARCELONATECH
Escola d'Enginyeria de Barcelona Est

13. Annex C

13.1. FEMM

LUA Scripts:

Optimization of Cogging Torque

```lua
--"Dibujo Rotor para Optimización - Variacíon de Alfa1"

open("Cogging Motor de Estudio SIN ROTOR.fem")
mi_saveas("SIM Cooging Optim.fem")

                            --ROTOR DRAW

--Angle (10 to 15)
interval=1;
p=5;
North=90;

for Alfa1=10,15, interval do

mi_addnode(0,39)

--Magnet:
mi_addnode(0,31.725)
mi_addnode(0,34.925)
mi_addnode(-8,31.725)
mi_addnode(-8,34.925)
mi_addsegment(0,31.725,-8,31.725)
mi_addsegment(-8,34.925,0,34.925)
mi_addsegment(-8,34.925,-8,31.725)

--Slot:
mi_addnode(0,31.65)
mi_addnode(0,35)
mi_addnode(-8.075,35)
mi_addnode(-8.075,31.65)
mi_addnode(-8.075,33.325)
mi_addnode(-10.275,33.325)
mi_selectnode(0,39)
mi_copyrotate(0,0,17.5,1,0)

--Alfa1 Point
mi_selectnode(0,39)
mi_copyrotate(0,0,Alfa1,1,0)

mi_addsegment(-8.075,31.65,0,31.65)
mi_addsegment(-8.075,31.65,-8.075,33.325)
mi_addsegment(-8.075,33.325,-10.275,33.325)
mi_addsegment(-8.075,35,0,35)
mi_addsegment(-10.275,33.325,-11.7,37.2)
--8.5,38--> Always the closest, no matter the angle increase
```

UNIVERSITAT POLITÈCNICA DE CATALUNYA
BARCELONA**TECH**
Escola d'Enginyeria de Barcelona Est

```
mi_addsegment(-8.075,35,-8.5,38)
mi_addarc(0,39,-11.7,37.2,17.5,1)
mi_selectarcsegment(-0.5,39)
mi_deleteselected()
--Mirror
mi_selectrectangle(-12.5,31,4,38.5,4)
mi_setgroup(99)
mi_selectrectangle(-12.5,31,4,38.5,4)
mi_mirror(0,0,0,40,4)
mi_selectnode(0,39)
mi_deleteselected()

--Materials
mi_getmaterial("Air")
mi_getmaterial("NdFeB 40 MGOe")
mi_getmaterial("Pure Iron")
mi_modifymaterial("Pure Iron",0,"Iron Rotor")
mi_modifymaterial("Iron Rotor",9,0)
mi_modifymaterial("Iron Rotor",8,0.98)
mi_modifymaterial("Iron Rotor",6,1)

--Air:
mi_addblocklabel(-9.6,39.8)
mi_selectlabel(-9.6,39.8)
mi_setblockprop("Air", 1, 0, 0, 0, 0, 0)
mi_clearselected()

mi_addblocklabel(-9.5,33.7)
mi_selectlabel(-9.5,33.7)
mi_setblockprop("Air", 1, 0, 0, 0, 99, 0)
mi_clearselected()

--Copyrotate
mi_selectgroup(99)
mi_copyrotate(0,0,36,9,4)

--Magnets:
mi_addblocklabel(0,33)
mi_selectlabel(0,33)
mi_setblockprop("NdFeB 40 MGOe",1,0,0,North,98,0)
mi_clearselected()

mi_addblocklabel(19.4,26.7)
mi_selectlabel(19.4,26.7)
mi_setblockprop("NdFeB 40 MGOe",1,0,0,(North-(360/(2*p))+180),98,0)
mi_clearselected()

mi_selectgroup(98)
mi_copyrotate(0,0,72,4,2)
mi_clearselected()

--Rest of parts
--Shaft
mi_addnode(-15,0)
mi_addnode(15,0)
mi_addarc(-15,0,15,0,180,1)
mi_addarc(15,0,-15,0,180,1)
mi_addblocklabel(0,2)
```

```
mi_selectlabel(0,2)
mi_setblockprop("<No Mesh>", 1, 0, 0, 0, 99, 0)
mi_clearselected()
--Out Diameter
mi_addnode(0,40)
mi_addnode(0,-40)
mi_addarc(0,40,0,-40,180,1)
mi_addarc(0,-40,0,40,180,1)
mi_addblocklabel(0,18)
mi_selectlabel(0,18)
mi_setblockprop("Iron Rotor", 1, 0, 0, 0, 99, 0)
mi_clearselected()
--Fixations
mi_addnode(-1.5,22.47)
mi_addnode(1.5,22.47)
mi_addarc(1.5,22.47,-1.5,22.47,180,1)
mi_addarc(-1.5,22.47,1.5,22.47,180,1)
mi_addblocklabel(0,22.47)
mi_selectlabel(0,22.47)
mi_setblockprop("<No Mesh>", 0, 0, 0, 0, 99, 0)
mi_clearselected()
mi_selectcircle(0,22.47,1.6,4)
mi_copyrotate(0,0,72,4,4)


--Group:99
mi_selectcircle(0,0,40.3,4)
mi_setgroup(99)
mi_clearselected()


                           --COGGING SIMULATION
  periode=360/10;
  step=periode/20;
  for deg=0, 2*periode, step do
    mi_analyze(1);
    mi_loadsolution();

    --cogging torque calculation routine
    mo_groupselectblock(99)
    cog=mo_blockintegral(22)  --(Steady-state weighted stress tensor
torque)
    mo_clearblock()
    mi_seteditmode("group")
    mi_selectgroup(99)
    mi_moverotate(0,0,step)

    --store on file
    handle=openfile("Cogging RESULTS.txt","a")
    write(handle,deg,"  ",cog,"  ","\n")
    closefile(handle)
    mo_close()
  end

mi_deletematerial("Air")
mi_deletematerial("NdFeB 40 MGOe")
mi_deletematerial("Iron Rotor")
mi_selectgroup(99)
mi_deleteselected()
end
```

UNIVERSITAT POLITÈCNICA DE CATALUNYA
BARCELONATECH
Escola d'Enginyeria de Barcelona Est

Fluxes- CEMF determination

```
--NO LOAD Simulation

mi_modifycircprop("A",1,0); --0 A Current
mi_modifycircprop("B",1,0);
mi_modifycircprop("C",1,0);
showconsole()
data={};
steps=40;
p=5;

--mechanical degrees increase
delta=(360/p)/steps;
for k=1,(steps+1) do
print((k-1).."/"..steps);
mi_analyze(1);
mi_loadsolution();
data[k]={};

--position in mechanical and electrical degrees
data[k][1]=(k-1)*delta;
data[k][2]=p*data[k][1];

--Data from circuits
ca,va,fa=mo_getcircuitproperties("A");
cb,vb,fb=mo_getcircuitproperties("B");
cc,vc,fc=mo_getcircuitproperties("C");
data[k][3]=fa;
data[k][4]=fb;
data[k][5]=fc;

--Motor rotation
mi_selectgroup(99);
mi_moverotate(0,0,delta,4);
mi_clearselected();
end

--store in file
fp=openfile("Resultados de flujo.txt","w");
for k=1,(steps+1) do
write(fp,data[k][1]," ",data[k][2]," ",data[k][3]," ",data[k][4],"
",data[k][5], "\n")
end
closefile(fp);
```

Delta Torque

```
--Delta Torque Simulation
p=5
periode=360/p
```

```
step=periode/20

for deg=0, 2*periode, step do

  mi_analyze(1)
  mi_loadsolution()

  --torque calculation routine
  mo_groupselectblock(99)
  MI=mo_blockintegral(22)--Steady-state weighted stress tensor torque
  mo_clearblock()

  --Motor rotation
  mi_selectgroup(99)
  mi_moverotate(0,0,step)

  --store on file
  handle=openfile("Resultados Par delta.txt","a")
  write(handle,deg,"    ",MI,"\n")
  closefile(handle)
  mo_close()
end
```

Rotating Torque

```
--Load Simulation
pi=3.1415926
p=5
periode=360/p
step=periode/20
Imax=7.283*sqrt(2)
alfa=0




for deg=0, 2*periode, step do

  --time variable currents
  Ia=Imax*cos(alfa*pi/180)
  Ib=Imax*cos(alfa*pi/180-2*pi/3)
  Ic=Imax*cos(alfa*pi/180+2*pi/3)
  mi_modifycircprop("A",1,Ia);
  mi_modifycircprop("B",1,Ib);
  mi_modifycircprop("C",1,Ic);

  mi_analyze(1)
  mi_loadsolution()

  --torque calculation routine
  mo_groupselectblock(99)
  MI=mo_blockintegral(22)--Steady-state weighted stress tensor torque
  mo_clearblock()
```

UNIVERSITAT POLITÈCNICA DE CATALUNYA
BARCELONATECH
UPC   Escola d'Enginyeria de Barcelona Est

```
  --Circuits properties
  ia,va,fa=mo_getcircuitproperties("A")
  ib,vb,fb=mo_getcircuitproperties("B")
  ic,vc,fc=mo_getcircuitproperties("C")
end

--Motor rotation
  mi_seteditmode("group")
  mi_selectgroup(99)
  mi_moverotate(0,0,step)
  alfa=alfa+p*step

  --store on file
  handle=openfile("Resultados Par girando.txt","a")
  write(handle, deg,"   ", MI,"   ", Ia," ", Ib," ", Ic,", ",\n")
  closefile(handle)
  mo_close()

end
```

Inductances: Ld and Lq determitaion

```
--Calculation of Ld and Lq with the Magnetic Field Energy

p=5
periode=360/p
step=periode/20

--File creation
handle=openfile("Results Magnetic Field Energy.txt", "a")
write(handle, "deg ", "Energy ", "\n")
closefile(handle)

for deg=0, 2*periode, step do

  mi_analyze();
  mi_loadsolution();

  handle=openfile("Results Magnetic Field Energy.txt","a")

  --select windings, PM+air and gap
  mo_groupselectblock(7)
  mo_groupselectblock(8)
  mo_groupselectblock(9)
  mo_groupselectblock(99)
  mo_groupselectblock(88)

  --Magnetic Field Energy
  E=mo_blockintegral(2)

  --Store in file
  write(handle,deg," ",E, "\n")
  closefile (handle)
  mo_close()
```

```
  --Motor rotation
  mi_seteditmode("group")
  mi_selectgroup(99)
  mi_selectgroup(70)
  mi_moverotate(0,0,step)
end
```

Iron losses

```
--Iron losses calculation
-- Static Method

freq=125
depth=0.09
--Bertotti Coefficients M470-50
Kc=0.542828
Kh=203.7494
Ka=8.351784


for deg=0, 2*periode, step do
  Pfes=0
  Pfer=0
  Ia=Imax*cos(alfa*pi/180)
  Ib=Imax*cos(alfa*pi/180-2*pi/3)
  Ic=Imax*cos(alfa*pi/180+2*pi/3)
  mi_modifycircprop("A",1,Ia);
  mi_modifycircprop("B",1,Ib);
  mi_modifycircprop("C",1,Ic);

  mi_analyze(1)
  mi_loadsolution()

    --Stator Losses
  mo_smooth("off")
  numelm=mo_numelements()

  for k=1, numelm do
  --properties of each element
  --p1, p2, p3: magnetic potencial in each triangle vertex
  --x,y: triangle center coordinates
  --a: element area
  --g:element group

  p1,p2,p3,x,y,a,g=mo_getelement(k)
  if (g==2) then
    --element volume
    dv=depth*a*mm^2
    --center properties
    a,bx,by,sig,e,hx,hy=mo_getpointvalues(x,y)
    Bx=abs(bx)
    By=abs(by)
```

UNIVERSITAT POLITÈCNICA DE CATALUNYA
BARCELONA**TECH**
Escola d'Enginyeria de Barcelona Est

```
    Bmod=sqrt(Bx^2+By^2)

    --LOSSES
    Pfes=Pfes+(Kh*freq*Bmod^2+Kc*(freq*Bmod)^2+Ka*(freq*Bmod)^1.5)*dv
  end

--Rotor losses
  --properties of each element
  --p1, p2, p3: magnetic potencial in each triangle vertex
  --x,y: triangle center coordinates
  --a: element area
  --g:element group
  p1,p2,p3,x,y,a,g=mo_getelement(k)

  if (g==99) then
    --element volumen
    dv=depth*a*mm^2
    --center properties
    a,bx,by,sig,e,hx,hy=mo_getpointvalues(x,y)
    Bx=abs(bx)
    By=abs(by)
    Bmod=sqrt(Bx^2+By^2)
    --LOSSES
    Pfer=Pfer+(Kh*freq*Bmod^2+Kc*(freq*Bmod)^2+Ka*(freq*Bmod)^1.5)*dv
  end
end
  mi_seteditmode("group")
  mi_selectgroup(99)
  mi_moverotate(0,0,step)
  alfa=alfa+p*step

  --store on file
  handle=openfile("Resultados pérdidas.txt","a")
  write(handle, deg,"  ", Pfes," ", Pfer, "\n")
  closefile(handle)
  mo_close()

end
```
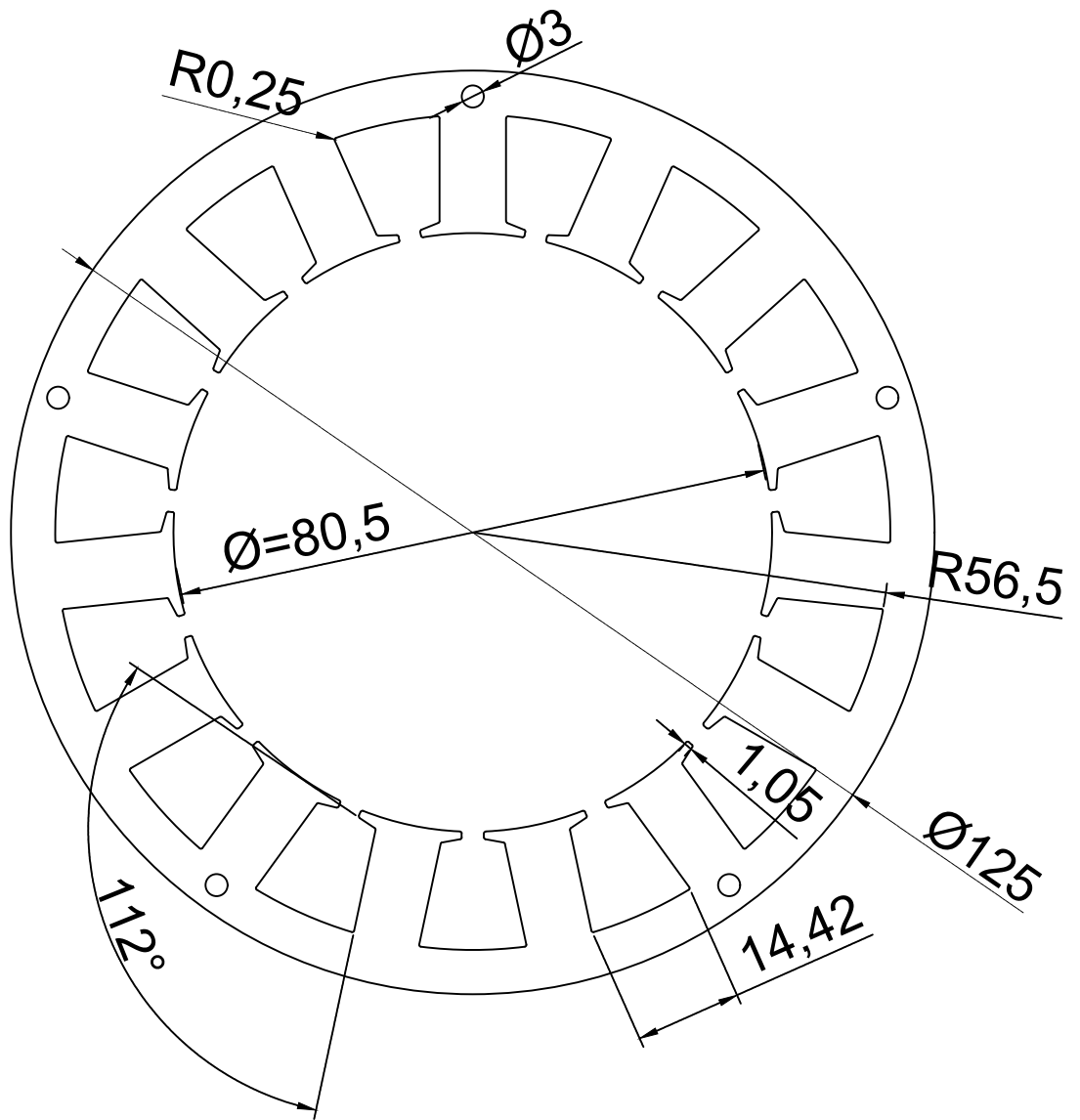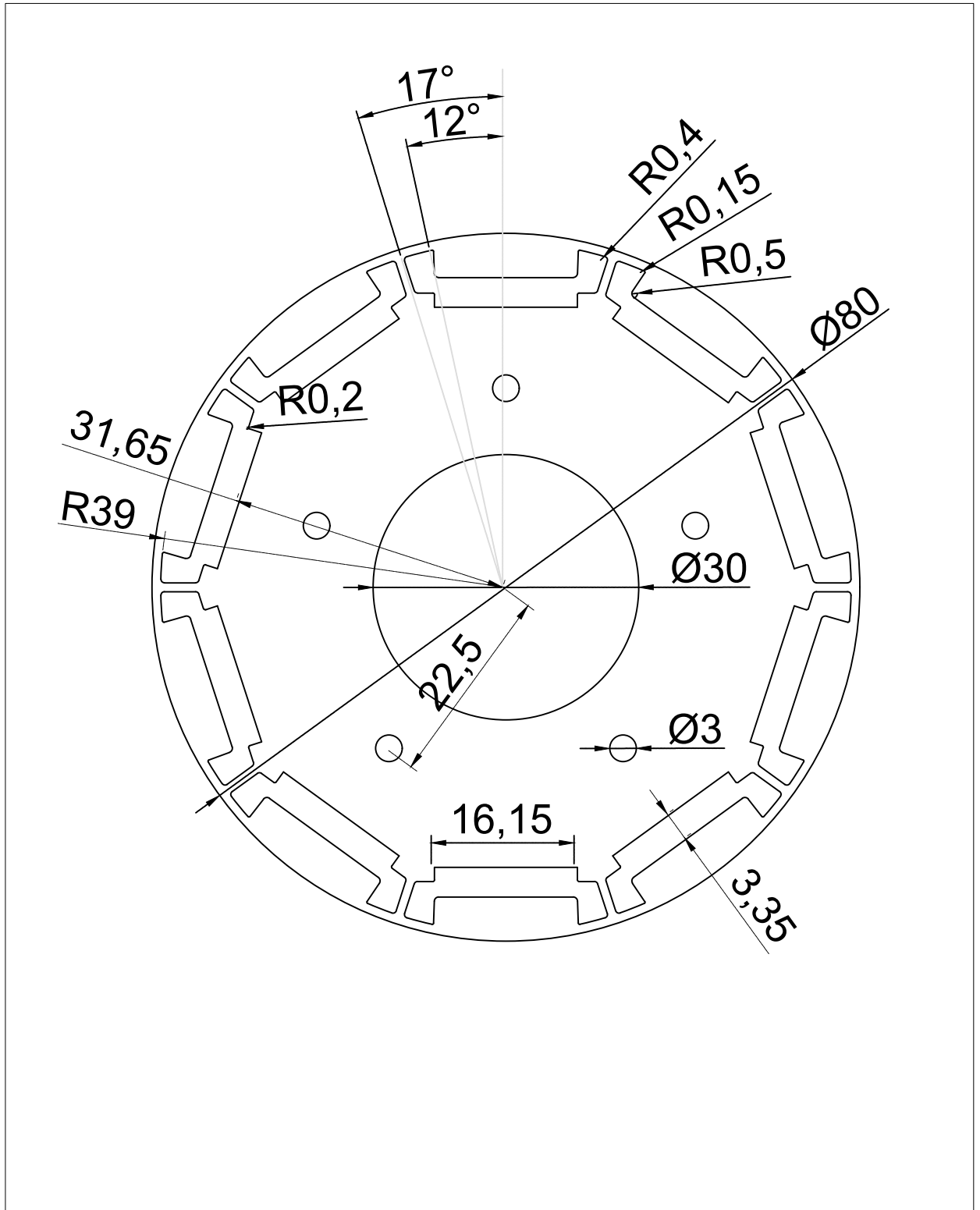
14. Annex D

14.1. Structure draws

R0,25

Ø3

Ø=80,5

R56,5

1,05

Ø125

112°

14,42

Draw 1		
Stator Armature D125 - 15 Slots		UNIVERSITAT POLITÈCNICA DE CATALUNYA BARCELONATECH Escola d'Enginyeria de Barcelona Est

Scale		Author
1:1	Motor: PMSM 2,2 kW	Matias Richter

mm	Material	Tolerances						Director
	Steel M470 50 A	Measure:	<3	÷6	÷30	÷120	÷400	÷1000	Ramón Bargalló Perpiñà
		Tolerance	0.1	0.1	0.2	0.3	0.5	0.8	

17°
12°
R0,4
R0,15
R0,5
Ø80
R0,2
31,65
R39
Ø30
22,5
Ø3
16,15
3,35

Draw 2			
Stator Armature D80 - 10 Poles		UNIVERSITAT POLITÈCNICA DE CATALUNYA BARCELONATECH	
		Escola d'Enginyeria de Barcelona Est	
Scale	Motor: PMSM 2,2 kW	Author	
3:2			Matias Richter
mm	Material	Tolerances	Director

mm		Material		Tolerances							Director	
		Steel M470 50 A		Measure:	<3	÷6	÷30	÷120	÷400	÷1000	Ramón Bargalló Perpiñà	
				Tolerance	0.1	0.1	0.2	0.3	0.5	0.8		

3,2

90

16

Draw 4

Machine Armature and PM

UNIVERSITAT POLITÈCNICA DE CATALUNYA
BARCELONATECH
UPC
Escola d'Enginyeria de Barcelona Est

Scale		Motor: PMSM 2,2 kW						Author	
1:1								Matias Richter	
mm	Material	Tolerances						Director	
		Measure: <3 ÷6 ÷30 ÷120 ÷400 ÷1000						Ramón Bargalló Perpiñà	
		Tolerance 0.1 0.1 0.2 0.3 0.5 0.8							